I. CHRONOPOTENTIOMETRY IN THIN LAYERS OF SOLUTION

II. APPLICATION OF THIN LAYER CHRONOPOTENTIOMETRY TO KINETIC STUDIES

III. PROTON SPIN RELAXATION IN HYDROGEN DEUTERIDE

Thesis by

Charles Richard Christensen

In Partial Fulfillment of the Requirements

For the Degree of

Doctor of Philosophy

California Institute of Technology

Pasadena, California

1966

(Submitted December 10, 1965)

To my father and mother

for their encouragement

ABSTRACT

Part I

The theory of chronopotentiometry of an electroactive species confined in a thin layer of solution next to the electrode is presented. The potential-time and transition time relationships are verified for the reduction of iron(III) in 1F perchloric acid for solution layer thicknesses from 2×10^{-3} to 1×10^{-2} cm. The technique is shown to be especially useful for studying irreversible systems that give poor diffusion chronopotentiograms and for determining the number of electrons transferred in electrochemical reactions. Application of the technique to the oxidation of N,N-dimethyl-p-phenylenediamine in 1F sulfuric acid is demonstrated.

Part II

A chronopotentiometric procedure is described for studying the rates of chemical reactions that occur subsequent to the electrochemical generation of a species that is confined in a thin layer of solution next to an electrode. The theory is verified for the hydrolysis of p-benzoquinoneimine, and the technique is shown to be especially useful for the study of reactions too slow to be investigated conveniently by other voltammetric methods. Applicability of the technique to the study of ligand exchange reactions is demonstrated.

Part III

The HD proton spin-lattice relaxation time T_1 has been measured in pure HD and in mixtures with eight other gases as a function of composition at room temperature. Probabilities per collision for Δm_J transitions are determined from the Schwinger relation and compared with the values for pure H_2 and H_2 in the same gases. The differences are interpreted in terms of the displacement of the HD center of mass from the charge center of the molecule, and show up in a way correlated with the strengths of the interactions. With the assumptions that ΔJ transitions do not contribute to the nuclear spin relaxation and that the isotropic part of the H_2 intermolecular interaction is described by the Lennard-Jones potential, it is found that the Bloom-Oppenheim theory does not explain the large difference in relaxation times for HD and H_2. A method of testing the form of isotropic intermolecular potential functions is proposed.

ACKNOWLEDGMENTS

I thank Professor Fred C. Anson for his help and guidance during the first years of my graduate study. I thank Professor Sunney I. Chan for his help and guidance during the past two years. Both of these gentlemen have given generously of their time for my education.

Thanks are also due to the other members of the faculty and graduate students who have taken time to answer questions and give their assistance on problems. The advice and help of Dr. O. Hayes Griffith is especially appreciated. Special mention is also due to Peter James Lingane and Dr. David E. Wood.

I thank my wife, Peggy, for her expert secretarial assistance while discharging her duties as wife and mother.

I am grateful to the California Institute of Technology and the National Science Foundation for financial support.

TABLE OF CONTENTS

I. CHRONOPOTENTIOMETRY IN THIN LAYERS OF SOLUTION

The theory of chronopotentiometry of an electroactive species confined in a thin layer of solution next to the electrode is presented. The potential-time and transition time relationships are verified for the reduction of iron(III) in 1F perchloric acid for solution layer thicknesses from 2×10^{-3} to 1×10^{-2} cm. The technique is shown to be especially useful for studying irreversible systems that give poor diffusion chronopotentiograms and for determining the number of electrons transferred in electrochemical reactions. Application of the technique to the oxidation of N,N-dimethyl-p-phenylenediamine in 1F sulfuric acid is demonstrated.

INTRODUCTION

In a previous study (1), electrodes made by sealing platinum wire into the end of a length of soft glass tubing were occasionally defective in that the glass was not bonded to the wire over the entire area of the seal, and a layer of solution of an electroactive species could be trapped between the glass and metal. If the exposed surface of the electrode was washed free of reactant and the electrode was placed in a deaerated solution of supporting electrolyte containing no dissolved reactant, chronopotentiograms corresponding to the reactant trapped in a thin layer next to the electrode could be obtained (1-3).

In this investigation two types of thin layer chronopotentiometric electrodes have been devised for which the dimensions of a layer of solution confined at its surface are known. The equations have been derived for the transition time and for the electrode potential as a function of time for these electrodes. These relations were tested and verified for the reduction of iron(III) in 1F perchloric acid. A comparison of the potential vs. time curves for thin layer chronopotentiometry of p-phenylenediamine and N,N-dimethyl-p-phenylenediamine has been made. The number of electrons involved in the oxidation of N,N-dimethyl-p-phenylenediamine in 1F sulfuric acid at platinum electrodes was determined to test the utility of the thin layer technique for the determination of n values.

EXPERIMENTAL

Apparatus. Two different types of electrodes were designed for thin layer chronopotentiometry. Wire electrodes consisted of a length of 0.030-inch diameter platinum wire sealed in 5-mm. soft glass tubing by heating in a flame (Figure 1A). Before sealing, the wire was electroplated with copper to a thickness of 1 to 1.5×10^{-3} cm. for a distance of 1 cm. from one end. The glass was fused around the wire to cover 5 mm. of the copper-coated section and 5 mm. of the adjacent clean platinum. The copper was removed from the wire by successive treatments with warm concentrated nitric and hydrochloric acids, and the wire protruding from the glass was cut off as close as possible to the end of the glass tube.

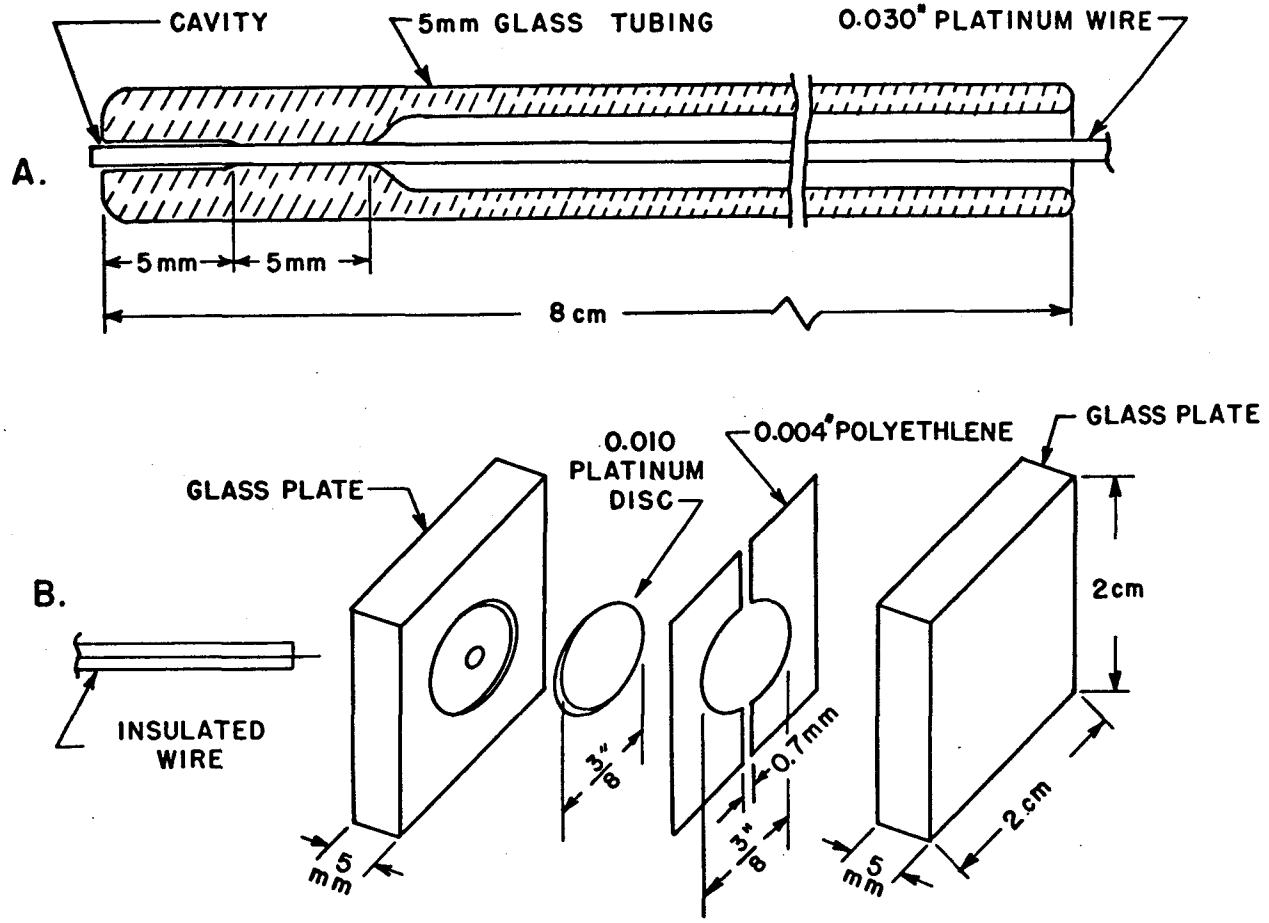

Figure 1. Electrodes for thin layer chronopotentiometry

A. Wire electrode

B. Plate electrode

A plate electrode was used in experiments where somewhat thicker layers of solution were desired. This electrode consisted of a 0.010-inch thick platinum disk 0.375 inch in diameter that was cemented with an epoxy resin (Resinweld Adhesive No. 4) into a hole in the face of a glass plate (Figure 1B). An insulated wire from the rear of the glass plate furnished the electrical connection. The electrode was held a uniform distance from a second glass plate by a 0.004-inch polyethylene gasket coated with silicone high vacuum grease. Two slits in the gasket, about 0.7 mm. wide, allowed electrical contact from the working electrode to the auxiliary and reference electrodes in the external solution and permitted the cavity to be filled with solution. Clamps held the two plates together.

The working electrode used in diffusion chronopotentiometry was a piece of platinum foil, 0.4 sq. cm. in area, welded to a platinum wire sealed in glass. A similar electrode with an area of 6.5 sq. cm. was used as the working electrode in the controlled potential electrolysis.

The chronopotentiometric circuit and instrumentation have been described (1). A commercial potentiostat and current integrator from Analytical Instruments Inc., Bristol, Conn., were employed in the large scale controlled potential electrolysis. The temperature of all solutions was within 2° of 24° C. Potentials were measured with respect to a calomel electrode saturated with sodium chloride but are reported vs. the usual potassium chloride-saturated calomel electrode.

Materials. Solutions of iron(III) were prepared by pipeting a sample of 0.1049F stock solution into a volumetric flask and diluting with 1F perchloric acid. The stock solution was prepared by dissolving reagent grade ferric sulfate in 1F perchloric acid and standardized with dichromate after reduction with stannous chloride. Commercial Matheson, Coleman, and Bell p-phenylenediamine and N,N-dimethyl-p-phenylenediamine sulfate were used without further purification. Solutions were prepared immediately before use by dissolving the required weight of sample in air-free 1F sulfuric acid.

Procedure. The wire electrodes for thin layer chronopotentiometry were cleaned before each trial by filling the cavities with sulfuric acid-dichromate cleaning solution. The cleaning solution was then completely removed by washing the electrodes in stirred 1F perchloric acid for 12 hours followed by chronopotentiometric reduction of the surface film of platinum oxides. The electrodes were then washed free of perchloric acid by immersion in stirred distilled water for 24 hours and dried for 15 to 30 minutes in vacuo at room temperature.

The wire electrode cavity was filled by using a vacuum desiccator which had a wire beam suspended from the lid. The beam had a magnet attached to one end and a counterweight attached to the other end. A shallow dish containing the solution to be used was placed in the desiccator and the electrode suspended from one end of the beam above the solution. The desiccator was evacuated to the vapor pressure of the solution and the electrode made to dip into the solution by manipula-

tion with a second magnet outside the desiccator. Atmospheric pressure was then applied.

After filling, the outside of the electrode was immediately rinsed with distilled water to remove excess solution and the electrode placed in the cell containing deaerated 1F perchloric acid for chronopotentiometry of iron(III) or 1F sulfuric acid for chronopotentiometry of p-phenylenediamine and N,N-dimethyl-p-phenylenediamine. The electrode potential was lowered to 0.0 volt vs. S.C.E. to reduce all oxygen in the cavity. In the case of the diamines any imine initially present was reduced with the oxygen. With iron the Fe(III) was completely reduced at this potential so that the resulting Fe(II) first had to be reoxidized to obtain a cathodic chronopotentiogram corresponding to the reduction of Fe(III).

The plate electrode cavity was filled by aspiration with the solution of iron(III) in 1F perchloric acid through one of the slits in the gasket. The electrode assembly was immersed with the reference and auxiliary electrodes in a large volume of the deaerated solution, and chronopotentiograms for reduction of the iron(III) in the cavity were recorded. The concentration of iron(III) in the solution outside the cavity was made the same as that inside to eliminate loss of iron (III) from the cavity by diffusion during the several hours required to record a series of chronopotentiograms. However, none of the iron(III) in the external solution was reduced during any single chronopotentiogram. After each trial, the iron(II) produced was repeatedly oxidized chronopotentiometrically until no anodic wave appeared. The next ca-

thodic chronopotentiogram was recorded after waiting 5 minutes for concentration irregularities in the cavity to disappear.

DISCUSSION

Consider the reduction of an electroactive species Ox confined between an electrode at the origin and an inert wall parallel to the electrode at a distance ℓ from the origin. If species Ox is reduced with a constant current density and edge effects are neglected, the concentration of Ox at the electrode can be evaluated by means of Laplace transform methods. A solution of an analogous problem in heat conduction has been given (4). The result is:

$$C_o(0,t) = C_o^{\circ} - \frac{i\ell}{nFAD}\left[\frac{Dt}{\ell^2} + \frac{1}{3} - \frac{2}{\pi^2}\sum_{k=1}^{\infty}\frac{1}{k^2}\exp\left(-\frac{Dk^2\pi^2 t}{\ell^2}\right)\right] \qquad (1)$$

where n, F, A, and D have their usual significance, $C_o(0,t)$ is the concentration of Ox at the electrode surface, C_o° is the initial concentration of Ox, i is the constant current, and t the time.

Another form of Equation 1 is (4):

$$C_o(0,t) = C_o^{\circ} - \frac{2it^{1/2}}{nFA\pi^{1/2}D^{1/2}} - \frac{4it^{1/2}}{nFAD^{1/2}}\sum_{k=1}^{\infty} i\mathrm{erfc}\,\frac{k\ell}{\sqrt{Dt}} \qquad (2)$$

For large values of ℓ Equation 2 reduces to the equation for conventional chronopotentiometry.

The transition time τ occurs when $C_o(0,t) = 0$. For transition times long enough so that $\ell^2 < \tau D$ the exponential terms in Equation 1 may be neglected and the expression for τ becomes:

$$\tau = \frac{nFA\ell C_o^o}{i} - \frac{\ell^2}{3D} \tag{3}$$

For a couple obeying the Nernst equation the potential-time relation of the chronopotentiogram is

$$E = E' + \frac{RT}{nF} \ln \frac{\tau - t + \frac{2\ell^2}{\pi^2 D} \sum_{k=1}^{\infty} \frac{1}{k^2} \exp\left(-\frac{Dk^2\pi^2 t}{\ell^2}\right)}{t + \frac{\ell^2}{3D} - \frac{2\ell^2}{\pi^2 D} \sum_{k=1}^{\infty} \frac{1}{k^2} \exp\left(-\frac{Dk^2\pi^2 t}{\ell^2}\right)} \tag{4}$$

assuming equal diffusion coefficients for the oxidized and reduced forms. E' is the formal potential of the oxidation-reduction couple. The term $\ell^2/3D$ and the exponential terms in Equation 4 can easily be made small with respect to t. In this case, $E = E'$ at $t = \tau/2$.

As in diffusion chronopotentiometry the oxidation of species R can be studied by reversing the direction of the current through the cell at or before the transition time. Inspection of Equation 3 shows that the second term on the right hand side can be neglected if ℓ is sufficiently small and the amount of species Ox in the cavity is sufficiently large. For example, if $\ell = 10^{-3}$ cm., and $D = 10^{-5}$ cm.^{2} second^{-1}, the second term is 3×10^{-2} second. Thus, for transition times larger than approximately 3 seconds, the second term is negligible. Equation 3 then reduces to Faraday's Law as applied in coulometry at constant current. Therefore the transition time for the reoxidation of species R will be equal to the initial transition time for reduction of species Ox if the same current is employed.

The form of Equation 3 suggests a method by which accurate n values for electrode reactions can be determined even when diffusion coefficients are unknown. Conditions are chosen so that $\ell^2/3D$ is negligible compared to the measured transition time. The electrode is calibrated by reducing or oxidizing a substance of known concentration and n value. The known solution is replaced with an unknown and the n value calculated from the concentration and calibration factor according to

$$\tau = \frac{nFA\ell C_o^o}{i} \qquad (5)$$

RESULTS

Reduction of Ferric Iron. Figure 2 illustrates a thin layer chronopotentiometric wave for the reduction of 0.01049F iron(III) in 1F perchloric acid using the wire cavity electrode. The wave for the reoxidation of the iron(II) is also shown. The average distance between the glass and the wire in the cavity of the electrode used was 2.3×10^{-3} cm. The equality of the cathodic and anodic transition times (28.9 vs. 29.3 second) is expected on the basis of Equation 3 and the small value of ℓ. Equation 4 predicts that for t large in comparison with $\ell^2/3D$, a plot of E vs. log $[(\tau - t)/t]$ for the cathodic process should be linear with a slope of 2.3 RT/nF. Logarithmic plots are shown in Figure 2 for the anodic and cathodic chronopotentiograms illustrated. The plots are linear in both cases. The slopes are 0.059 volt and 0.060 volt for the anodic and cathodic waves, respectively, both of which agree well with the theoretical value of 0.059 volt.

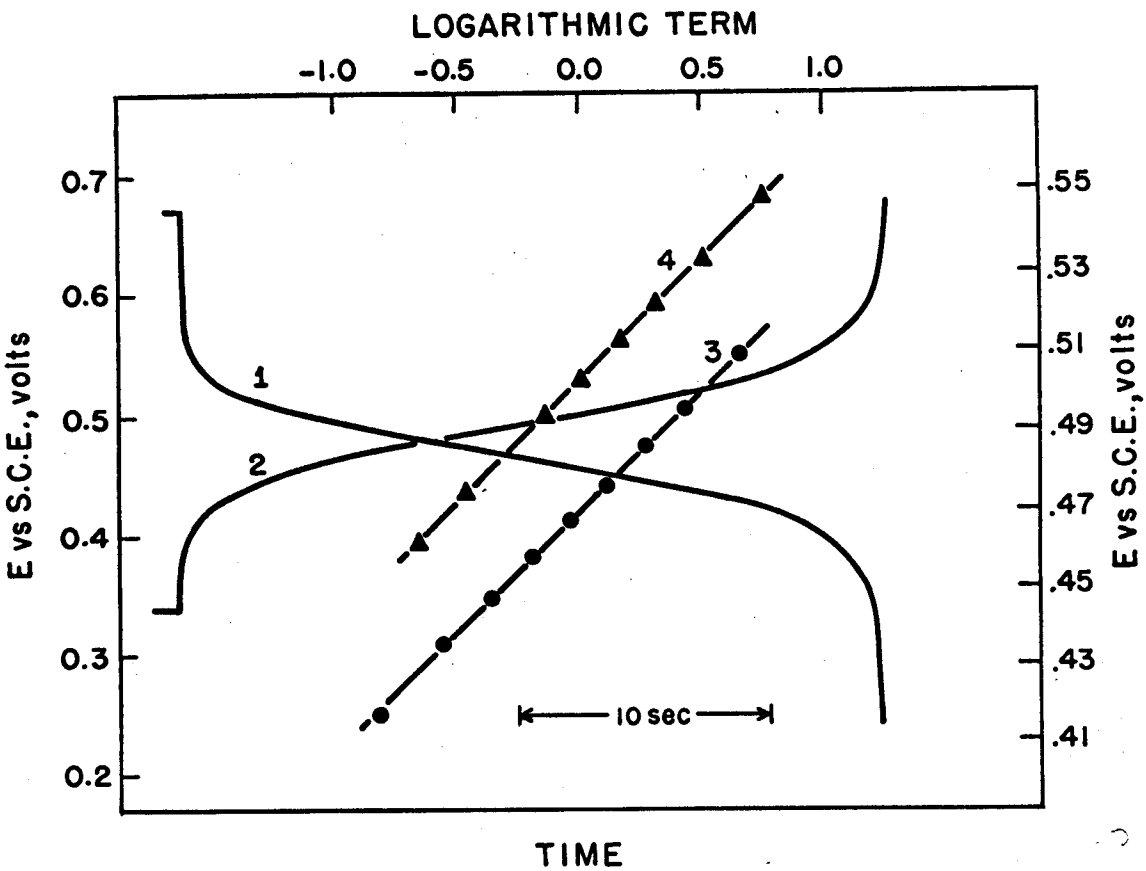

Figure 2. Thin layer chronopotentiograms for Fe(III) and their corresponding logarithmic plots

1. Reduction of 0.01049F Fe(III) in 1F $HClO_4$
2. Reoxidation of Fe(II) after recording curve 1
3. E vs. log $[(\tau - t)/t]$ for curve 1
4. E vs. log $[t/(\tau - t)]$ for curve 2

Potential scale for logarithmic plots is on the right

The reproducibility of filling the cavity next to the electrode is indicated by the data for the reduction of iron(III) shown in Table I. The values are shown for the transition times (τ_{Fe}) measured for each wire electrode in three trials using 0.01049F iron(III) in 1F perchloric acid and a current of 10.4 μa. The average deviation is less than 2% for each of the five electrodes. The differences among the electrodes arise from variations in cavity volumes.

TABLE I. Electrode Calibration and Determination of n Value for the Oxidation of N,N-Dimethyl-p-phenylenediamine[a]

Electrode	τ_{Fe} (sec.)	Mean τ_{Fe} (sec.)	τ_{DPP} (sec.)	n
1	13.0 13.7 13.4	13.4	12.9	2.02
2	16.8 17.1 17.3	17.1	16.1	1.99
3	19.9 20.4 20.3	20.2	19.1	2.00
4	28.2 28.6 28.2	28.3	26.0	1.94
5	26.3 27.2 27.2	26.9	24.2	1.90
			Mean	1.97
			Rel. std. dev.	2.5%

[a] 10.49×10^{-3}F Fe(III) in 1F $HClO_4$. 4.95×10^{-3}F N,N-Dimethyl-p-phenylenediamine in 1F H_2SO_4.

The agreement among the various electrodes in Table I and the correct slopes of the logarithmic plots in Figure 2 demonstrate that there is no significant nonuniformity of current density over the electrode surfaces. In 0.2F perchloric acid the electrolyte resistance was sufficiently increased, so that discrepancies arising from ohmic potential differences within the cavity could be detected.

Diffusion of iron(III) from the electrode cavity into the surrounding solution caused the transition times to become gradually shorter during the recording of successive chronopotentiograms in iron-free supporting electrolyte. However, the percentage of iron(III) diffusing from the cavity in the minute or two required to record the first reduction wave was negligible.

Chronopotentiometry of iron(III) in 1F perchloric acid using the plate electrode tested the validity of Equations 3 and 4 under conditions such that the term $\ell^2/3D$ and the exponential terms were not negligible. The layer thickness ℓ was about 1.3×10^{-2} cm. Transition times, measured over a wide range of current densities, are shown plotted vs. 1/i in Figure 3. The good linearity of this plot indicates that Equation 3 is obeyed. A plot of E vs.

$$\log \frac{\tau - t + \frac{2\ell^2}{\pi^2 D} \sum_{k=1}^{\infty} \frac{1}{k^2} \exp\left(-\frac{Dk^2\pi^2 t}{\ell^2}\right)}{t + \frac{\ell^2}{3D} - \frac{2\ell^2}{\pi^2 D} \sum_{k=1}^{\infty} \frac{1}{k^2} \exp\left(-\frac{Dk^2\pi^2 t}{\ell^2}\right)}$$

for a chronopotentiometric wave for iron(III) reduction obtained with this electrode is also shown in Figure 3. The value of 8.4 seconds for

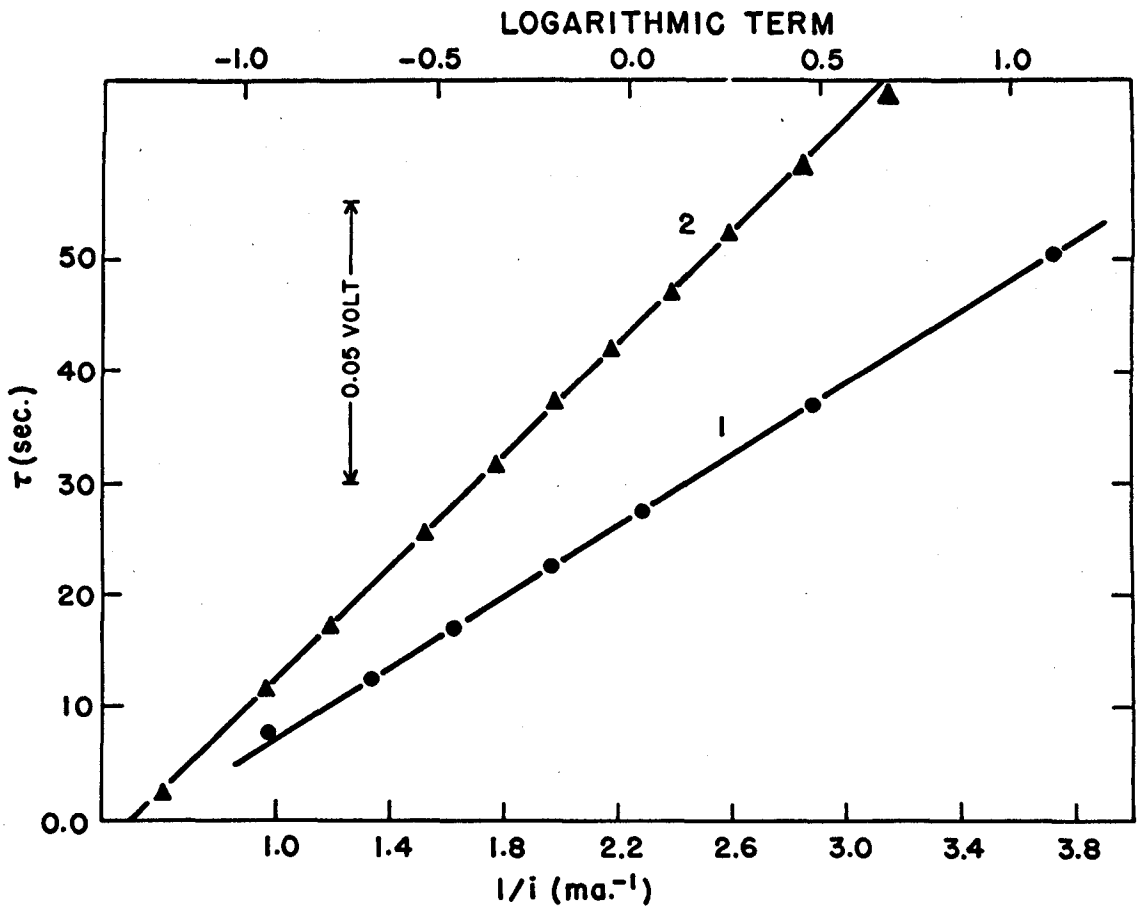

Figure 3. Chronopotentiometry of Fe(III) using electrode in Figure 1B

1. Variation of τ with 1/i for 0.0210F Fe(III) in 1F $HClO_4$
2. E vs. the logarithmic term in Equation 4 for τ = 37.0 sec. The logarithmic scale at the top and potential scale in the inset correspond to line 2

$\ell^2/3D$ obtained from the intercept of line 1 was used in this logarithmic plot. Agreement with Equation 4 is demonstrated by the linearity of line 2 and its slope of 0.064 volt. This slope presumably is somewhat higher than that obtained with the smaller cavities because of higher currents needed and the possibility of less uniform current distribution over the electrode surface.

Comparison of Thin Layer and Diffusion Chronopotentiograms. A comparison of potential-time curves for thin layer chronopotentiometry and diffusion chronopotentiometry of p-phenylenediamine (Figure 4) and N,N-dimethyl-p-phenylenediamine (Figure 5) demonstrates advantages of thin layer chronopotentiometry in the study of irreversible electrode reactions. Wire electrodes were used to obtain the thin layer chronopotentiograms. The concentrations are approximately 5×10^{-3}F and the transition times are similar for the four curves in Figures 4 and 5. Although none of the waves is completely reversible, note the sharper potential inflection at the transition time and the improvement in reversibility in the chronopotentiograms for the thin layer compared to those for diffusion. This improvement results because the current density required for a given transition time in the thin layer case is much smaller than that which would be required for the same transition time in diffusion chronopotentiometry with the same concentration of the oxidizable species. In the examples shown the current density for the solution layer case is about one sixth as large as that used to obtain the diffusion chronopotentiograms.

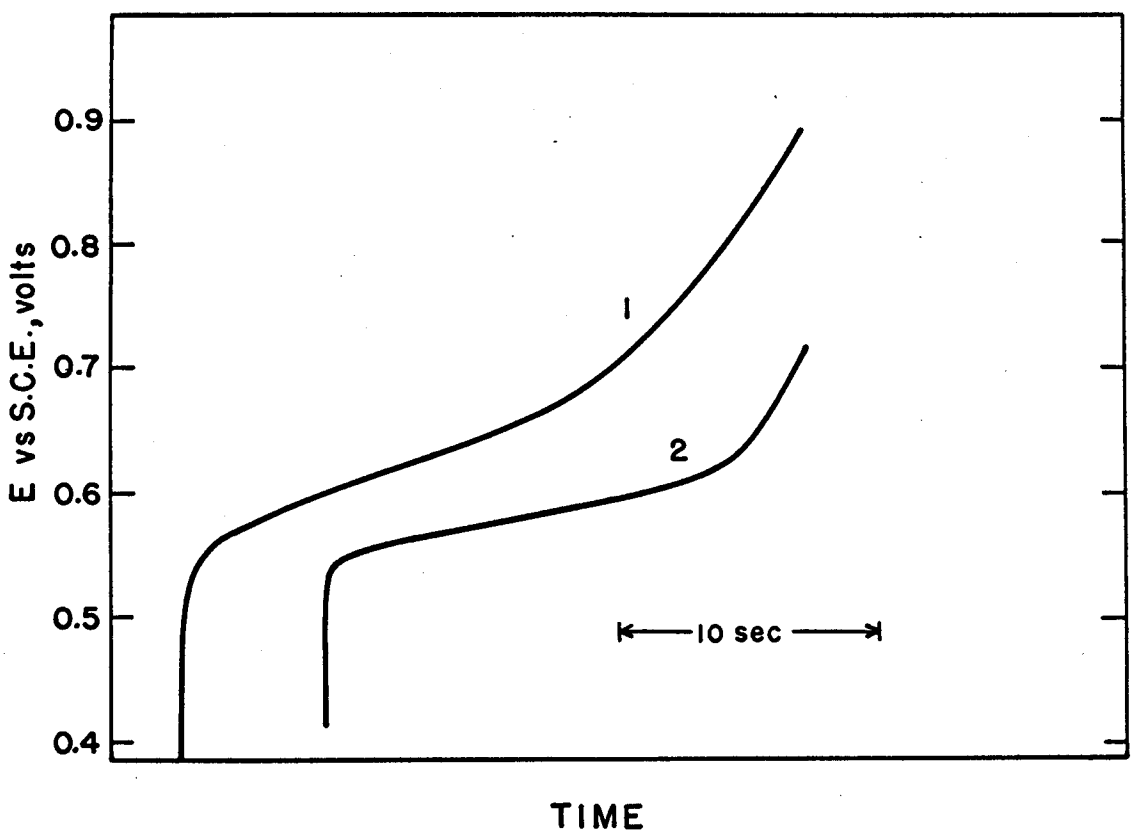

Figure 4. Chronopotentiograms for oxidation of p-phenylenediamine

1. Diffusion chronopotentiometry of 4.72×10^{-3}F solution; current density, 0.6 ma. $cm.^{-2}$
2. Thin layer chronopotentiometry of 4.99×10^{-3}F solution; current density, 0.09 ma. $cm.^{-2}$

Supporting electrolyte, 1F H_2SO_4

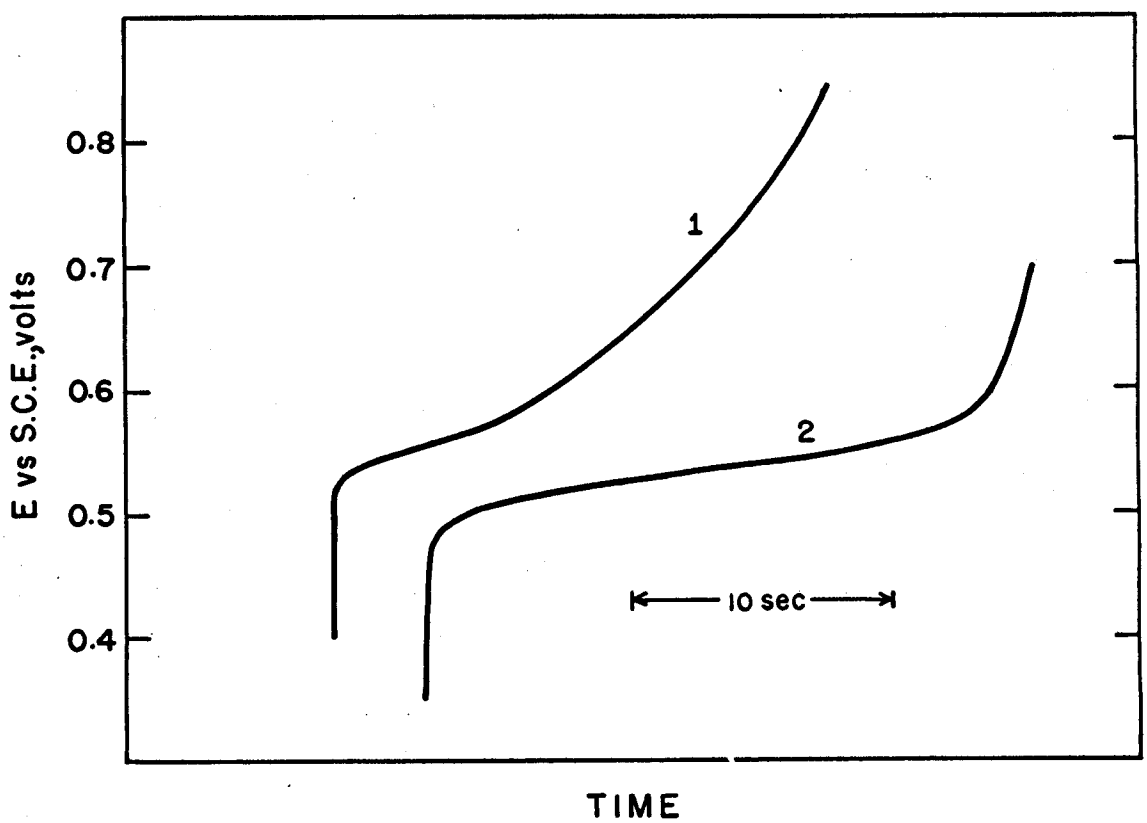

Figure 5. Chronopotentiograms for oxidation of N,N-dimethyl-p-phenylenediamine

1. Diffusion chronopotentiometry of 4.95×10^{-3}F solution; current density, 0.6 ma. $cm.^{-2}$
2. Thin layer chronopotentiometry of 4.95×10^{-3}F solution; current density, 0.09 ma. $cm.^{-2}$

Supporting electrolyte, 1F H_2SO_4

A sharper potential inflection occurs at the transition time in the thin layer chronopotentiograms because, once all the reactant in the cavity is oxidized, all the current is available for the next electrode reaction, the oxidation of water. In the diffusion chronopotentiograms a major fraction of the current continues to be consumed by the oxidation of the reactant which diffuses to the electrode following the transition time. There is thus less current available to oxidize water and the potential changes less rapidly.

Determination of the n value for Oxidation of N,N-dimethyl-p-phenylenediamine. The oxidation of N,N-dimethyl-p-phenylenediamine may occur in the following steps:

$$H_2N—C_6H_4—N(CH_3)_2 - e \rightleftharpoons [H_2N—C_6H_4—N(CH_3)_2]^+$$

$$[H_2N—C_6H_4—N(CH_3)_2]^+ - e \rightleftharpoons NH{=}C_6H_4{=}N(CH_3)_2^+ + H^+$$

Relatively little work has been reported on the voltammetry of N,N-dimethyl-p-phenylenediamine. A chronopotentiometric investigation of the oxidation of N,N-dimethyl-p-phenylenediamine at platinum electrodes in acid solution by Kuwana (6) indicated a two-electron reaction. However, further chemical reactions of the oxidation products complicated the interpretation of the results.

Table I summarizes the results of the determination of the n value for N,N-dimethyl-p-phenylenediamine oxidation in 1F sulfuric acid. The cavities of five wire electrodes were calibrated by thin layer chronopotentiometry of iron(III) in 1F perchloric acid. The transition times (τ_{DPP}) for thin layer chronopotentiometry of 4.95×10^{-3}F N,N-

dimethyl-p-phenylenediamine in 1F sulfuric acid were then measured for each electrode at the same current density. The transition times were taken as the time required for the electrode potential to reach 0.30 volt vs. S.C.E. and 0.65 volt vs. S.C.E. in the reduction of iron(III) and the oxidation of N,N-dimethyl-p-phenylenediamine, respectively. The n values were calculated from the transition time and concentration ratios according to Equation 5. The experimental mean value of 1.97 is in good agreement with the value of 2 expected for the oxidation of N,N-dimethyl-p-phenylenediamine to the diimine.

To compare this value with that obtained by conventional controlled potential electrolysis, the n value for N,N-dimethyl-p-phenylenediamine oxidation in 1F sulfuric acid was determined by controlled potential coulometry at a platinum electrode held at a potential of 0.68 volt vs. S.C.E. The electrolysis was stopped when the current had decreased to 3% of its original value and was approximately constant. The number of coulombs which had passed corresponded to an n value of 2.36. High n values are frequently obtained in controlled potential electrolysis of organic substances; they have been attributed to complex reactions between intermediate electrode reaction products and the starting material, producing substances which can be further oxidized to cause the stoichiometry of the reaction to become complicated (5). This difficulty is largely eliminated in thin layer chronopotentiometry.

Application to Kinetics Studies. The thin layer technique is well suited to the study of chemical reactions coupled to the electrochemical reaction. For example, if species A is not electroactive, but

in slow equilibrium with an electroactive species B, the complete oxidation of species B in the electrode cavity would lead to a transition time corresponding to the equilibrium amount of B initially present. If the current is turned off for a measured time and then a second anodic chronopotentiogram recorded, the transition time would be a measure of the rate at which A is converted to B.

LITERATURE CITED

(1) Anson, F. C., Anal. Chem., 33, 1498 (1961).

(2) Ibid., p. 1838.

(3) Anson, F. C., J. Am. Chem. Soc., 83, 2387 (1961).

(4) Carslaw, H. S., Jaeger, J. C., "Conduction of Heat in Solids," 2nd ed., p. 112, Oxford Univ. Press, London, 1959.

(5) Galus, Z., White, R. M., Rowland, F. S., Adams, R. N., J. Am. Chem. Soc., 84, 2065 (1962).

(6) Kuwana, Theodore, Ph.D. Thesis, University of Kansas, Lawrence, Kan., (1957).

II. APPLICATION OF THIN LAYER CHRONOPOTENTIOMETRY TO KINETIC STUDIES

A chronopotentiometric procedure is described for studying the rates of chemical reactions that occur subsequent to the electrochemical generation of a species that is confined in a thin layer of solution next to an electrode. The theory is verified for the hydrolysis of p-benzoquinoneimine, and the technique is shown to be especially useful for the study of reactions too slow to be investigated conveniently by other voltammetric methods. Applicability of the technique to the study of ligand exchange reactions is demonstrated.

INTRODUCTION

The preceding paper described a technique for performing chronopotentiometric experiments with the electroactive species confined in a thin layer of solution next to the electrode (2). The present investigation demonstrates the applicability of the technique to the study of the kinetics of chemical reactions following electron transfer. The hydrolysis rate of p-benzoquinoneimine in acidic solutions and the rate of attack of nickel(II) ion on (ethylenediaminetetraaceto)cobaltate(II) (CoY^{-2}) were studied.

Diffusion chronopotentiometry with current reversal (9) and other voltammetric techniques (5,10) have been used to study the decomposition of the product of an electrochemical reaction. All such techniques are limited to systems for which the rate of chemical reaction is relatively rapid (half lives no greater than about 30 seconds)

in order to detect appreciable reaction before the electrolysis product diffuses away from the electrode. In thin layer chronopotentiometry, the species are confined at the electrode so that this difficulty is avoided and accurate measurements of considerably smaller rate constants can be carried out. An analogous approach that involved adsorption of electroactive organic compounds on carbon black was recently reported by Voorhies (11).

EXPERIMENTAL

Apparatus and Procedure. The electrodes used consisted of 0.030-inch diameter platinum wire sealed in 5-mm. soft glass tubing with a cavity 5 mm. long and 2×10^{-3} cm. thick between the wire and the glass. These were constructed as previously described (2). The chronopotentiometric circuitry was standard (7).

The procedure followed in cleaning and filling the electrodes has been described (2). A fresh sample of the p-aminophenol solution was used to fill each electrode. The electrode potential was forced to 0.1 volt vs. SCE to reduce the oxygen and any p-benzoquinoneimine or p-benzoquinone initially present. The small amount of hydroquinone present after this initial reduction was then oxidized chronopotentiometrically to ensure 100% current efficiency for the subsequent oxidation of p-aminophenol. The hydroquinone oxidation wave overlaps the p-aminophenol wave so that some p-aminophenol was oxidized along with the hydroquinone. The small amount of p-benzoquinoneimine that resulted was quickly reduced before significant hydrolysis had occurred and the

current was turned off when the potential reached 0.48 volt so that no reduction of p-benzoquinone occurred. The confined solution was now ready for the anodic and cathodic chronopotentiograms to be recorded to measure the hydrolysis rate.

In the study of the CoY^{-2}-Ni^{+2} reaction, the solution pH was 3.0 and the electrode potential had to be forced to -0.2 volt vs. SCE to reduce the oxygen in the cavity. The CoY^{-} was also reduced at this potential so the resulting CoY^{-2} was reoxidized before final chronopotentiograms were recorded. A current of 10 μa. was employed in all trials.

The cell with auxiliary and reference electrodes contained a deaerated solution with none of the electroactive species but otherwise identical to that in the electrode cavity. The cell temperature was within 0.1° of the stated temperature.

Materials. Eastman White Label p-aminophenol was recrystallized twice from water under nitrogen for the experiments in 1.017F sulfuric acid. The material used in 0.510F sulfuric acid was further purified by sublimation at 110° in vacuo (3). Solutions were prepared immediately before use by dissolving the required weight of sample in the air-free sulfuric acid solution. The acid solutions were prepared by dilution of standardized 4.066F sulfuric acid. Triply distilled water was used to prepare all solutions in the experiments with p-aminophenol.

Barium (ethylenediaminetetraaceto)cobaltate(III) was prepared by the procedure in "Inorganic Synthesis" (4). A stock solution of the potassium salt was prepared by treating a solution of the barium salt

with a slight excess of K_2SO_4. Other chemicals were reagent grade and were used without further purification.

RESULTS AND DISCUSSION

p-Benzoquinoneimine Hydrolysis. The anodic oxidation of p-aminophenol in aqueous solutions has been studied by several workers (6, 8, 9). The reactions involved are reported to be

$$HO{-}C_6H_4{-}NH_2 - 2e \rightleftharpoons O{=}C_6H_4{=}NH + 2H^+$$

$$O{=}C_6H_4{=}NH + H_2O \longrightarrow O{=}C_6H_4{=}O + NH_3$$

The equations for thin layer chronopotentiometry reduce to those for coulometry at constant current under conditions such that $\ell^2/3D \ll t$, where ℓ is the layer thickness, D is the diffusion coefficient of the electroactive species, and t is the time from the start of electrolysis (2). For oxidation of p-aminophenol for time t_f and interruption of current flow for time t_d, the transition time, τ, for reduction of the remaining p-benzoquinoneimine is shown in Appendix I to be given by

$$\tau = \frac{1}{k} \ln \left[1 + e^{-kt_d}(1 - e^{-kt_f})\right] \qquad (1)$$

in which k is the pseudo first-order rate constant for the irreversible reaction and the same current is employed for anodic and cathodic processes.

Figure 1 shows a typical thin layer chronopotentiometric wave for oxidation of p-aminophenol and for subsequent reduction of p-benzoquinoneimine and p-benzoquinone. An anodic transition time would be

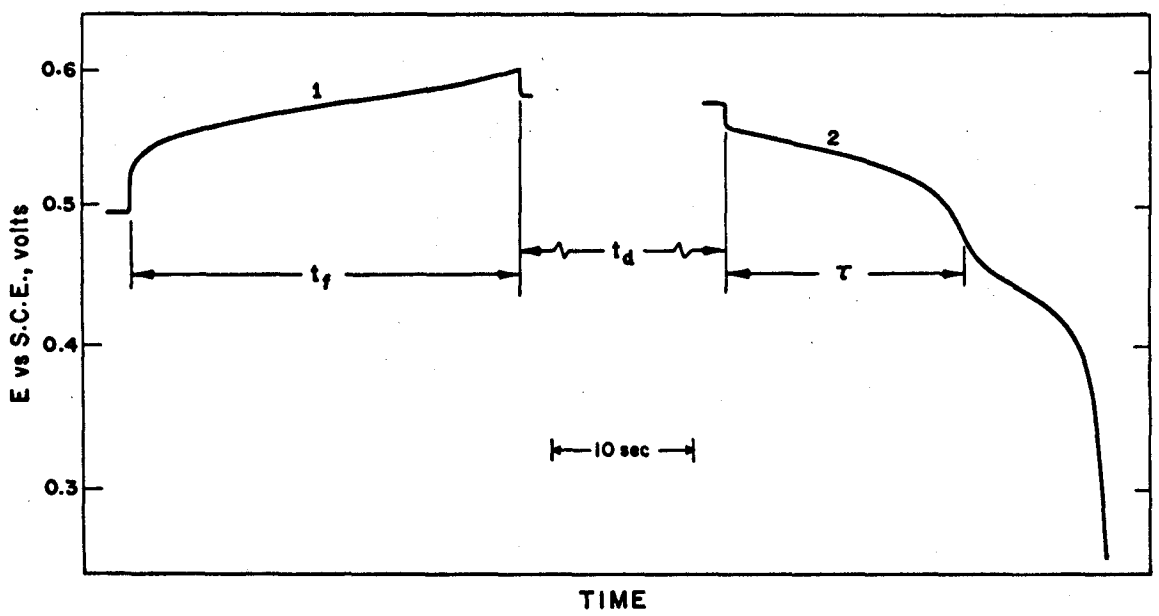

Figure 1. Thin layer chronopotentiograms obtained with 1.01×10^{-2}F p-aminophenol (1.017F H_2SO_4, 25.0° C., t_d = 45.4 sec.)

1. Oxidation of p-aminophenol

2. Reduction of p-benzoquinoneimine and p-benzoquinone

obtained if the current had not been turned off. The first cathodic wave corresponds to p-benzoquinoneimine reduction (8, 9). Data were obtained for a series of electrodes over a wide range of t_d, and k was calculated for each trial by iterative solution of Equation 1 using a digital computer. The results are shown in Table I.

The agreement in k over the large range of t_d confirms the validity of Equation 1. The value of 0.027 ± 0.001 sec.$^{-1}$ for the rate constant in 0.510F sulfuric acid at 30.0° C. compares favorably with the value of 0.032 ± 0.005 sec.$^{-1}$ determined by Testa and Reinmuth (9) who used diffusion chronopotentiometry with current reversal. The errors given are standard deviations.

In the estimation of rate constants by diffusion chronopotentiometry with current reversal the parameter of interest is the difference between the observed length of the reverse wave for the reacting species and the value it would have had in the absence of any chemical reaction. As the rate constant becomes smaller, the magnitude of this difference approaches the error in the measurement of the reverse transition time, introducing a large error in the measured value of k (9). In thin layer chronopotentiometry, this error is made much smaller by interrupting the current for time t_d at the end of the forward electrolysis time and waiting for the chemical reaction to proceed extensively before measuring the reverse transition time. In this way very small rate constants can be measured by simply increasing the waiting time.

In diffusion chronopotentiometry with current reversal, the length of the reverse wave for a chemically reacting species is always less than one third of the forward wave. In thin layer chronopotentiom-

TABLE I. Specific Reaction Rate for the Pseudo First-Order Hydrolysis of p-Benzoquinoneimine

A. 30.0°C., 0.510F H_2SO_4, 1.01×10^{-2}F p-aminophenol				B. 25.0°C., 1.017F H_2SO_4, 1.01×10^{-2}F p-aminophenol			
t_f, sec.	t_d, sec.	τ, sec.	$k \times 10^3$, $sec.^{-1}$	t_f, sec.	t_d, sec.	τ, sec.	$k \times 10^3$, $sec.^{-1}$
14.0	0.0	10.1	27.8	32.1	9.9	23.9	7.8
14.4	0.0	10.6	24.7	40.3	13.2	28.8	7.1
24.5	0.0	14.5	27.4	41.8	19.9	28.1	7.3
40.1	0.0	18.9	26.7	17.5	24.3	13.0	7.5
30.6	5.5	15.3	25.2	24.6	24.7	17.4	7.6
30.1	6.7	14.4	26.2	24.9	33.5	16.1	8.1
32.8	9.6	13.5	27.9	19.0	42.2	12.7	7.0
16.7	13.4	8.4	26.7	27.4	45.4	16.6	7.5
34.7	14.7	12.6	27.5	36.0	50.4	20.3	7.3
32.3	18.9	11.4	26.3	29.1	51.4	17.1	7.2
30.3	21.0	10.5	26.1	16.6	51.1	10.3	7.4
16.4	21.7	7.1	25.5	30.4	57.6	16.7	7.4
13.5	22.3	5.6	27.7	27.0	59.1	15.4	7.0
22.2	24.6	7.9	26.6	29.6	62.5	15.8	7.4
29.9	30.4	8.3	26.4	40.3	63.5	20.1	7.4
25.2	31.7	7.3	26.3	39.0	70.7	19.0	7.3
13.9	32.3	4.6	26.7	22.9	74.8	11.7	7.3
37.2	40.6	7.3	26.7	35.7	76.7	16.3	7.6
				40.6	80.8	18.6	7.1
				26.5	91.6	11.9	7.3
		Mean	26.6			Mean	7.4
		Std. dev.	0.8			Std. dev.	0.2

etry, however, the reverse wave will be longer because all (instead of only about one third) of the unreacted electrolysis product reaches the electrode during the reverse transition time. Relative errors in the measurement of reverse transition times are thus reduced and increased accuracy in the calculated values of k results.

The utility of thin layer chronopotentiometry for measurement of a rate constant too small to be measured conveniently by diffusion chronopotentiometry is shown by the data in Table 1B for the hydrolysis of p-benzoquioneimine at 25.0° in 1.017F sulfuric acid. The relative standard deviation of the results under these conditions is approximately the same as for the reaction at 30.0° in 0.510F sulfuric acid. A typical experimental error in the measurement of τ was about 3%, which would cause a 4 to 6% error in k.

The sum of the reverse transition times for both waves was not equal to the oxidation time as theoretically expected, but was from 4 to 8% less in 1.017F sulfuric acid and from 2 to 4% less in 0.510F sulfuric acid. No more than a 2 to 3% decrease can be attributed to diffusion of the oxidized species out of the cavity so that this discrepancy may be due to a slow reaction of p-benzoquinoneimine to form an electrochemically inert product. Similar behavior has been observed in constant current coulometry of p-aminophenol adsorbed on carbon black (11).

Substitution Reaction between Nickel(II) and CoY^{-2}. The rate of attack of nickel(II) cation on cobalt(II)-EDTA anion, CoY^{-2}, was also

investigated with thin layer chronopotentiometry. The chemical reaction involved is:

$$CoY^{-2} + Ni^{+2} \longrightarrow NiY^{-2} + Co^{+2}$$

in which CoY^{-2}, Ni^{+2}, and Co^{+2} represent all forms of the corresponding species in solution.

Pseudo first-order rate constants were determined for the reaction of CoY^{-2} in 0.36F $NiSO_4$ at 25.0° C. The solution was buffered at pH 3.0 with 0.40F phosphate buffer. The CoY^{-2} was generated in the electrode cavity by reduction of 1.0×10^{-2}F CoY^{-} which is a substitution-inert complex. The solution contained 0.50F NaBr to increase the reversibility of the CoY^{-2} oxidation (1). The experiment consisted of generating CoY^{-2} for a measured time, t_f, turning off the current for time, t_d, and then reversing the direction of current flow and recording an anodic chronopotentiogram corresponding to the amount of CoY^{-2} which had not reacted with the excess Ni^{+2} ion. The results are shown in Table II.

The absence of variations in k over the wide range of t_d confirms the assumption that the reaction is first order in $[CoY^{-2}]$. The large standard deviation in k and the occasional values of k as much as 70% higher than the mean may indicate catalysis of the exchange reaction by the platinum electrode surface.

TABLE II. Pseudo First-Order Rate Constant for Nickel Attack on CoY^{-2}[a]

t_f, sec.	t_d, sec.	τ, sec.	$k \times 10^3$, $sec.^{-1}$
12.4	0.0	10.9	11.0
16.7	0.0	13.8	12.8
16.1	9.3	11.9	13.0
10.6	20.1	7.8	10.7
15.2	27.2	10.3	9.8
10.0	29.6	5.7	15.3
13.0	29.7	7.4	14.4
11.8	29.8	7.4	11.9
13.6	32.6	8.4	11.2
11.3	40.1	5.8	13.9
12.6	43.7	6.3	13.0
12.6	49.5	5.3	14.8
15.4	57.4	5.5	15.1
18.0	60.5	7.6	11.7
		Mean	12.8
		Std. Dev.	1.7

[a] 25.0°C., pH 3.00, 0.36F $NiSO_4$, 0.40F phosphate buffer, 0.50F NaBr, 1.0×10^{-2}F KCoY.

LITERATURE CITED

(1) Anson, F. C., J. Electrochem. Soc., 110, 436 (1963).

(2) Christensen, C. R., Anson, F. C., Anal. Chem., 35, 205 (1963).

(3) Dunn, S. A., J. Am. Chem. Soc., 76, 6191 (1954).

(4) "Inorganic Syntheses," Therald Moeller, ed., Vol. 5, p. 186, McGraw-Hill, New York, 1957.

(5) Kemula, W., Kublock, Z., Roczniki Chem., 32, 941 (1958).

(6) Knobloch, E., Collection Czech. Chem. Commun., 14, 508 (1949).

(7) Lingane, J. J., "Electroanalytical Chemistry," 2nd ed., Chap. XXII, Interscience, New York, 1958.

(8) Snead, W. K., Remick, A. E., J. Am. Chem. Soc., 79, 6121 (1957).

(9) Testa, A. C., Reinmuth, W. H., Anal. Chem., 32, 1512 (1960).

(10) Vlcek, B., Collection Czech. Chem. Commun., 25, 668 (1960).

(11) Voorhies, J. D., Davis, S. M., J. Phys. Chem., 67, 332 (1963).

III. PROTON SPIN RELAXATION IN HYDROGEN DEUTERIDE

The HD proton spin-lattice relaxation time T_1 has been measured in pure HD and in mixtures with eight other gases as a function of composition at room temperature. Probabilities per collision for Δm_J transitions are determined from the Schwinger relation and compared with the values for pure H_2 and H_2 in the same gases. The differences are interpreted in terms of the displacement of the HD center of mass from the charge center of the molecule, and show up in a way correlated with the strengths of the interactions. With the assumptions that ΔJ transitions do not contribute to the nuclear spin relaxation and that the isotropic part of the H_2 intermolecular interaction is described by the Lennard-Jones potential, it is found that the Bloom-Oppenheim theory does not explain the large difference in relaxation times for HD and H_2. A method of testing the form of isotropic intermolecular potential functions is proposed.

INTRODUCTION

The fluctuating magnetic fields at spin $\frac{1}{2}$ nuclei determine the rate at which the nuclear spin system approaches thermodynamic equilibrium with its surroundings. The rate at which the magnetization M_z of the nuclear spin system approaches its equilibrium value M_o is usually exponential. The time constant T_1 for the decay is known as the longitudinal or spin-lattice relaxation time. The x- and y-components, M_x and M_y, each decay to zero with a time constant, T_2, called the transverse or spin-spin relaxation time. This is the characteristic time in which the individual precessing nuclear spins lose phase coherence.

The fluctuating magnetic fields possess, x-, y-, and z-components, H_x, H_y, and H_z. The magnetization M_z is affected by the Fourier components of H_x and H_y near the Larmor frequency, ω_o; these Fourier components induce transitions between the nuclear spin states. If the correlation time, τ, for the molecular reorientation is of the order of $1/\omega_o$ the spectral density at ω_o is a maximum and T_1 is a minimum. For longer or shorter correlation times the density at ω_o decreases and T increases. In the same way, the component H_x or H_y perpendicular to M_y or M_x also causes changes in that component of magnetization. In addition, H_z contributes to the decay of M_y and M_x. The field component, H_z, can be in the direction of the static field, H_o, or opposed to H_o causing the precession for the individual spins to be faster or slower than ω_o. Thus M_x and M_y will decay even in a rigid lattice where there are effectively no fluctuations. As the correlation time becomes shorter, or molecular motion becomes more

rapid, the H_z experienced by a given nucleus may change many times as the spin precesses and the dephasing takes place by a random walk. When molecular motion is very rapid, such that the field at a nucleus changes many times during a single rotation of the dipole in its precession ($1/\tau \gg \omega_o$), the precessing nuclear spin experiences equivalent fluctuating fields in the x-, y- and z-directions and the mechanism for M_x and M_y decay is the same as that for M_z decay. In this limit then $T_1 = T_2$.

These local fields experienced by a nucleus may arise from within the same molecule or from other nearby molecules. In gases such as molecular hydrogen, methane, etc. at low densities the contribution of intermolecular fields to relaxation is negligible. The important intramolecular fields in these gases are those due to the molecular rotation and the magnetic dipole moment of the other nuclei in the molecule. In the absence of intermolecular collisions these intramolecular fields remain well defined. However, when frequent collisons occur they are modulated by molecular reorientations. The Fourier components of the fluctuating fields at the proton Larmor frequency induce nuclear spin transitions and provide the mechanism for relaxing the nuclear spin system. Nuclear spin relaxation times in gases therefore depend upon the rate at which the molecules undergo transitions between rotational states. Changes in the rotational states require angular momentum transfer so that relaxation time measurements provide information on the anisotropic interactions between molecules.

Several other methods may be used to study the orientation dependent part of the intermolecular forces. The absorption of high frequency sound has been employed to study collision induced rotational transitions in molecular hydrogen (1) and mixtures of O_2 and N_2 with He (2). Thermal transpiration studies can provide similar information (3). A disadvantage of techniques such as these is that the measured quantity depends primarily on the isotropic interactions so that the percent error in the determination of the anisotropic contributions may be very large. In nuclear magnetic resonance studies the experimental conditions may readily be chosen such that the relaxation time depends only on the anisotropic interactions. Line broadening in rotational spectra (4 Chap. 13) can also be used although absorption spectroscopy is ordinarily limited to molecules with permanent dipole moments. Line width measurements in Raman spectra (5, 6) can provide the detailed time dependence of the rotational correlation function. Measurements of nuclear spin relaxation times provide only the (time) integral of the correlation function. In the techniques discussed above the pertinent rotational transitions are those between J states. For spin relaxation measurements in H_2 and possibly other molecules the important transitions are those between the m_J states within the J manifolds. The most detailed information on intermolecular interactions can be obtained from molecular beam experiments in which the beam is limited to a particular rotational state before collision and analyzed for specific states after collision (7). However these experiments are difficult,

especially if the beam intensity is reduced by rejecting all molecules except those in certain rotational states.

The present work is concerned with proton spin relaxation in hydrogen gas. A proton in a hydrogen molecule in a magnetic field may be described by the spin Hamiltonian (8, p. 316)

$$\hbar^{-1}\mathcal{H} = \omega_H I_{z1} + \gamma_H H' \underset{\sim}{I_1} \cdot \underset{\sim}{J}$$

$$+ \gamma_H H'' [\underset{\sim}{I_1} \cdot \underset{\sim}{I_2} - 3(\underset{\sim}{I_1} \cdot \underset{\sim}{n})(\underset{\sim}{I_2} \cdot \underset{\sim}{n})] \qquad (1)$$

where I_1 is the spin of the proton of interest, I_2 is the spin of the other nucleus, $\omega_H = -\gamma_H H_o$ is the proton Larmor frequency in the applied field H_o, H' is the spin-rotation coupling constant, $H'' = \gamma_2\hbar/2R^3$ is the dipolar coupling constant, and $\underset{\sim}{n}$ is the unit vector along the vector $\underset{\sim}{R}$ connecting the two nuclei. Molecular beam experiments have provided accurate values for H' and H'' (9).

Proton spin relaxation in H_2 gas has been investigated as a function of temperature, pressure, ortho-para ratio, and impurity concentration (10-15). It was found that T_1 is proportional to the gas density at low pressures. At high pressures the density approaches that of a liquid and T_1 increases more rapidly with increasing density. The reorientation probability per collision for collisions with spherically symmetric molecules or atoms is less than that for collisions with molecules of lower symmetry. The temperature dependence of T_1 is also different for H_2 at infinite dilution in gases of spherically symmetric and nonspherically symmetric molecules. The relaxation time for

H_2 in gases, such as N_2 increases as the temperature is decreased at constant density, but in symmetrical gases such as He and A, T_1 decreases with decreasing temperature to ca. 80°K then rapidly increases.

A theory for nuclear spin relaxation in H_2 was developed by Schwinger (16, 8 Chap. VIII) and extended by Needler and Opechowski (17) and Johnson and Waugh (12). This relates T_1 to the correlation times or the lifetimes of the molecules in the rotational states. The theory explains the proportionality of T_1 to the gas density but cannot account for the temperature dependence of T_1 or the different reorientation probabilities for collisions of H_2 with other gases. Bloom and Oppenheim have developed a more detailed theory for nuclear spin relaxation which relates the correlation times directly to intermolecular interactions (18, 19) and the theory has been applied to the interpretation of relaxation times for pure H_2, D_2, and H_2 with other gases (20). They obtained good agreement with the experimental data.

This investigation was undertaken to further test these theories by applying them to proton spin relaxation in HD. The HD molecule is of interest because of the rotational level spacing, the possibility of observing nuclear magnetic resonance for all the rotational states, the different contributions of the spin-rotational and dipole-dipole interactions to relaxation in H_2 and HD, and the displacement of the molecular center of mass from the charge center. The rotational level spacings are large for both HD and H_2 but in H_2 the levels between which transitions can occur are much more widely separated than in HD due to the smaller mass of H_2 and the symmetry restriction on the wavefunction.

The even rotational states in H_2, with total nuclear spin quantum number zero, are unobservable in nuclear magnetic resonance. In HD ca. 90% of the contribution to the proton relaxation time is due to the spin-rotational interaction, but in H_2 it contributes only ca. 40% and the dipole-dipole interaction is primarily responsible for relaxation. The displacement of the HD molecular center of mass from the charge center provides an accurate monitor of the details of the isotropic intermolecular potential.

THEORY

Before discussing the experimental results the theory for proton spin relaxation in hydrogen gas will be examined. Some generalizations on the correlation times and correlation functions are considered; the results of the Schwinger theory, generalized by Needler and Opechowski, and Johnson and Waugh are given; the results of the Bloom-Oppenheim theory are discussed; the strong collision limit is considered; and averaging of the relaxation time over the rotational states is also discussed.

Correlation Times and Correlation Functions. The relaxation of the nuclear spin system in gases is treated by time dependent perturbation theory using the density matrix method (21). The Hamiltonian in Eq. 1 consists of the Zeeman interaction perturbed by the time-dependent spin-rotational and dipole-dipole interaction. This perturbation, describing the interaction of the spin system with the "lattice" is written as a sum of products of lattice operators with operators depending

on the nuclear spin coordinates. In gases these lattice operators are the rotational angular momentum operators. The random fluctuations of these operators are described by their correlation functions which can usually be taken as exponential.

The symmetry of the interaction Hamiltonian allows T_1 to be described by only two correlation times. The Hamiltonian may be written as the sum of products of spherical irreducible tensors involving space and spin coordinates. The spin-rotation interaction is linear in the components of rotational angular momentum and transforms under coordinate rotations as a first-rank tensor (vector). The dipole-dipole part of the Hamiltonian transforms as a second-rank tensor. In general a different correlation time can be assigned to each component of the tensors. However the Larmor frequency ω_J is much smaller than the rate of collisions which change the orientation of J and the direction of J remains essentially unchanged between collisions. Therefore the J dependence of the correlation times depends only on the rank of the interaction and is independent of the type of interaction (12).

It should also be noted that the cross-correlation terms between the spin-rotational and dipole-dipole interactions in the relaxation matrix elements vanish because these are of different rank (22,23).

The molecular reorientations may involve changes in the rotational quantum number J or changes in m_J within a J manifold. For H_2 and HD, under conditions such that the inverse of the correlation times are much smaller than the rotational level spacings, the contribution of ΔJ transitions to the spin relaxation matrix elements is much less than

the contribution of Δm_J transitions (22, 17). Thus the correlation functions may be calculated by considering only matrix elements within each J manifold.

The assumption that the correlation functions are exponential has been justified by Bloom and Oppenheim (19) for gases in the weak collision limit.

Review of the Theories. The time rate of change of the components of the spin magnetization may be obtained from Redfield's differential equations for the elements of the density matrix (21, 24). The generalized Schwinger formula is obtained using simple exponential correlation functions with correlation times τ_ℓ^J. For H_2 under the usual experimental conditions (pressure $\gtrsim$ 1 atm) such that $\omega_o \tau_\ell^J \ll 1$ the relaxation times $T_{1,J}$ and $T_{2,J}$ are equal and for a molecule in rotational state J (16, 8 Chap. VIII, 17)

$$\frac{1}{T_{1,J}} = \frac{2}{3}\gamma_H^2 H'^2 J(J+1)\tau_1^J + \frac{6\gamma_H^4\hbar^2 J(J+1)}{R^6(2J-1)(2J+3)}\tau_2^J \qquad (2)$$

Similarly the proton relaxation time in HD is given by (12)

$$\frac{1}{T_{1,J}} = \frac{2}{3}\gamma_H^2 H_H'^2 J(J+1)\tau_{1,HD}^J + \frac{8\gamma_H^2\gamma_D^2\hbar^2 J(J+1)}{3R_{HD}^6(2J-1)(2J+3)}\tau_{2,HD}^J \qquad (3)$$

and accurate values for the coupling constants are available (25).

The Bloom-Oppenheim theory was also developed using the spin density matrix method. However rather than assuming a particular form,

they derived the correlation functions from first principles and related them to the intermolecular interactions.

In this theory it is assumed that the translational motion of the molecules is determined by the isotropic interactions alone, and these are described by Lennard-Jones potentials. The anisotropic part of the interaction Hamiltonian, $\mathcal{H}_R$, is taken as

$$\mathcal{H}_R = \mathcal{H}_R^{(1)} + \mathcal{H}_R^{(2)} \tag{4}$$

where $\mathcal{H}_R^{(1)}$ describes the interaction between a molecule in state J and a spherically symmetric molecule or atom. For H_2

$$\mathcal{H}_R^{(1)} = b^{(1)}(r)\, P_2(\cos\theta) \tag{5}$$

where r is the distance between the charge centers of the two molecules, θ is the angle between the axis of the H_2 molecule and $\underset{\sim}{r}$, and $P_2(\cos\theta)$ is the second degree Legendre polynomial.

The function $b^{(1)}(r)$ is taken to be similar to the Lennard-Jones potential with an attractive part proportional to $1/r^6$ and a repulsive part proportional to $1/r^n$. The best fit to the experimental results for pure H_2 could be obtained using

$$b^{(1)}(r) = 1.94 \times 10^{-15} \text{ erg } [0.74\ (a/r)^{19} - (a/r)^6] \tag{6}$$

where a is a characteristic length for the spherically symmetric interaction between two molecules. However, a purely repulsive function with $n \approx 19$ fits the data for pure H_2 almost as well as Eq. 8 and the experi-

mental data for H_2 in rare gases are adequately described by functions of the form

$$b^{(1)}(r) = k/r^{19} \tag{7}$$

Thus the form of $b^{(1)}(r)$ is not rigorously determined.

The interaction $\mathcal{H}^{(2)}(r)$ depends on the orientations of both molecules. If the interaction between H_2 and a gas X is taken to be the interaction between the quadrupole moments, Q, of the molecular charge distributions

$$\mathcal{H}_R^{(2)} = b^{(2)}(r) \sum_{\eta=-2}^{+2} a_\eta Y_2^\eta(\Omega_H) Y_2^{\eta*}(\Omega_X) \tag{8}$$

in which $b^{(2)}(r) = 4\pi\, Q_H\, Q_X/r^5$, $a_o = 6$, $a_1 + a_{-1} = -4$, $a_2 = a_{-2} = 1$, the Y_2^η are spherical harmonics, and Ω_H and Ω_X are the orientations of the symmetry axes of the molecules with respect to $\underset{\sim}{r}$.

Oppenheim and Bloom derived general expressions for the correlation functions in terms of the intermolecular potentials. They found that at pressures less than a few hundred atmospheres the correlation functions should be exponential. Using the Hamiltonians 5 and 8 the relaxation time for H_2 may be expressed in the form of Eq. 2 with the correlation times given by

$$\tau_1^J = \frac{(2J-1)(2J+3)\hbar^2}{2\rho a^4 (2\pi\beta\mu)^{\frac{1}{2}}} \left[\frac{6}{5}\pi I^{(1)}(2) + 0.134\, CI^{(2)}(4) \right]^{-1} \tag{9}$$

$$\tau_2^J = \frac{(2J-1)(2J+3)}{3(4J^2+4J-7)}\,\tau_1^J \qquad (10)$$

where ρ is the number density of the molecules X, $\beta = 1/kT$, $\mu = m_H m_X/(m_H+m_X)$, m_H and m_X are the masses of the molecules H and X respectively, and C is given by

$$C = \frac{5}{2}\sum_J P_J^X \frac{J(J+1)}{(2J-1)(2J+3)} \qquad (11)$$

in which P_J^X is the fraction of X molecules in rotational state J. The integral $I^{(q)}(p)$ is given by

$$I^{(q)}(p) = \int_0^\infty dy\left[\int_0^\infty [g(u)]^{\frac{1}{2}}\, u^{3/2} b^{(q)}(au)\, J_{p+\frac{1}{2}}(uy)\, dx\right]^2 \qquad (12)$$

where $u = r/a$, $g(u)$ is the radial distribution function for the H_2 -X pair interacting with a spherically symmetric potential, and $J_{p+\frac{1}{2}}(uy)$ is the Bessel function of order $p+\frac{1}{2}$.

Strong Collision Limit. Both the theories discussed above assume that the collisions are "weak," i.e., the rotational transition probabilities per collision are small. The condition for "strong" collisions is that a molecule in a given rotational state J will have an equal probability of being in any state m_J after the collision (26, 4 p. 338). Nuclear magnetic double resonance experiments for HD in CO_2 (22) and nuclear spin relaxation measurements for H_2 in CO_2 (12) indicate that collisions are strong in these cases. If the collisions are weak the correlation times depend on the rotational transformation

properties of the different interactions causing spin relaxation, but for strong collisions $\tau_1^J = \tau_2^J$. If it is also assumed that for strong collisions the correlation time is independent of J (22)

$$\tau_1^J = \tau_2^J = \tau \tag{13}$$

Average Relaxation Time. At room temperature more than one rotational state is populated and if the mean time for transitions between different J states, τ_J, satisfies the condition $\tau_1^J \ll \tau_J \ll T_{1,J}$ the observed relaxation time is (26, 19)

$$\frac{1}{T_1} = \sum_J P_J \frac{1}{T_{1,J}} \tag{14}$$

where (27)

$$P_J = \frac{(2J-1)\ \exp\ [-J(J+1)\hbar^2/2I_o kT]}{\sum_J (2J+1)\ \exp\ [-J(J+1)h^2/2I_o kT]} \tag{15}$$

is the probability that a J state is occupied. This result is analogous to that obtained for rapid chemical exchange (28) where the fractional populations of different nuclear sites replace P_J and the lifetimes of nuclei on the sites are required to be short compared with the inverse of the difference in chemical shift between the sites. Because of the symmetry of the wave functions, ortho hydrogen only occupies the odd rotational states (27) and the sum in Eqs. 14 and 15 is

taken over J = 1, 3, 5 ··· . Para hydrogen, with I = 0, is unobservable in nuclear magnetic resonance. In HD the relaxation time is averaged over all rotational states.

EXPERIMENTAL

All relaxation times were determined from the linewidths of the resonance signals under slow passage conditions using the relation $T_2 = (\pi \Delta \nu)^{-1}$, where $\Delta \nu$ is the full width at half height. The measured linewidths were corrected for saturation and overlap of adjacent lines in the HD triplet (Appendix II). These corrections were less than 3% in all cases. Saturation corrections were made by applying the relation (8 p. 47)

$$\frac{\Delta \nu'}{\Delta \nu} = \left(1 + \gamma_H^2 H_1^2 T_1 T_2\right)^{\frac{1}{2}} \qquad (16)$$

where $\Delta \nu'$ is the width of the line broadened by saturation. The spectrometer rf field control was calibrated by saturating a Fe^{+3} doped water sample for which $T_1 = 0.14$ sec. and assuming $T_1 = T_2$ (16). Spectra were recorded with a Varian A-60 spectrometer using audio frequency sideband calibration. Relaxation times less than ca. 25 msec. could not be measured because of decreased signal intensity and overlap of adjacent lines, while magnetic field inhomogeneity limited measurements to relaxation times less than ca. 100 msec. All measurements were made at 29 ± 1°C. It was necessary to spin the sample tubes to avoid magnetic

field inhomogeneity broadening (see Appendix III).

The progressive-saturation method was used to obtain T_1 for the sample of 50.5% HD in CO_2 by measuring the linewidths as the spectrometer rf field was progressively increased. It was found that $T_1 = 0.74\ T_2$. Within the accuracy of this technique (29) this confirms our assumption that $T_1 = T_2$.

In preparing the samples, the gases were first mixed in a bulb of known volume at a total pressure of ca. 300 mm Hg. The composition was determined by measuring the pressure with a mercury manometer after addition of each component. The samples were condensed into calibrated 5 mm standard wall Pyrex tubes (0.8 mm wall thickness) by immersion in liquid helium, and the tubes sealed with a torch. The total gas density in all samples was 25.0 amagats. After sealing each sample tube, the pressure in the mixing bulb was measured with a thermocouple gauge to confirm that all gas was condensed. Some sample tubes with 1.5 mm walls were used in preliminary experiments at pressures up to 90 atm., but these sometimes exploded due to strain in the glass at the end sealed with the torch.

The HD was made by reaction of General Dynamics 99.5% D_2O with Metal Hydrides, Inc., $LiAlH_4$ in n-butyl ether at 0°C. using the procedure described by Fookson, Pomerantz, and Rich (30). Air was removed from the $LiAlH_4$ slurry by three or four cycles of freezing the slurry, evacuating the system, and allowing the ether to thaw. The D_2O was added dropwise to the reaction flask as the slurry and ice bath surrounding the flask were stirred with a magnetic stirrer. After puncturing

the rubber septum it was covered with a few drops of D_2O to exclude air. A Vigreux column cooled with dry ice and a liquid nitrogen cold trap were placed between the reaction flask and the collecting bulbs. The gas used to prepare the samples was passed through another liquid nitrogen cold trap before introduction into the mixing bulb. The apparatus is shown in Fig. 1. Mass spectrometric analysis showed the gas to be 97.6% HD, 1.7% H_2 and 0.7% D_2. The analysis was made with the mass spectrometer inlet system at room temperature. The other gases used were obtained from Matheson and are listed in Table I.

TABLE I. Description of Gases

Gas	Purity %	Grade
H_2	99.95	Prepurified
D_2	99.5	
CH_4	99.0	C. P.
C_2H_6	99.0	C. P.
N_2	99.996	Prepurified
$CClF_3$	99.0	
CHF_3	98.0	
CO_2	99.99	Coleman

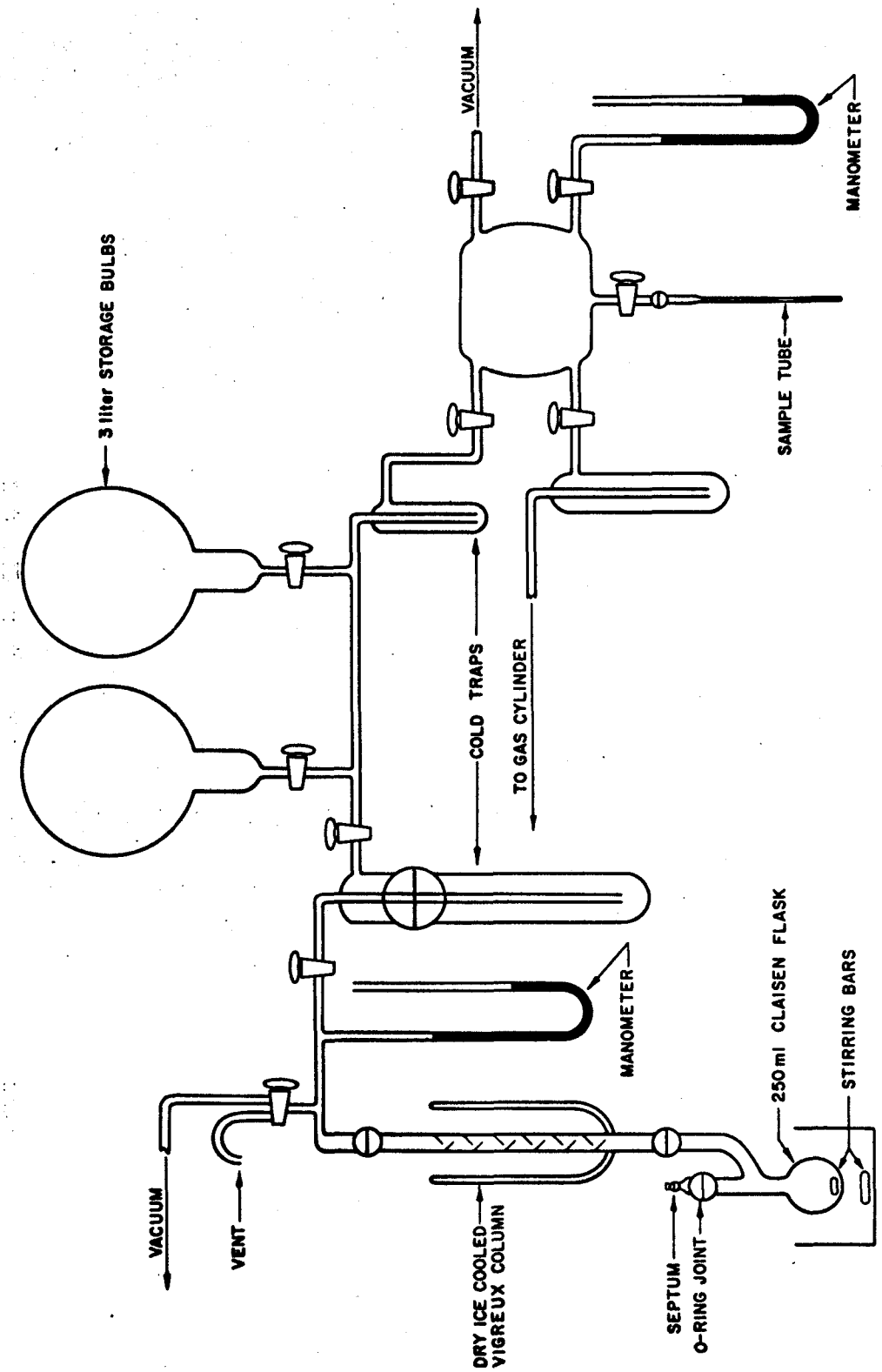

Fig. 1. Apparatus used to synthesize HD and prepare samples of HD mixed with other gases

RESULTS AND DISCUSSION

The proton spin relaxation time for HD was studied in pure HD and HD in eight different buffer gases. Measurements were made using pure HD, and HD in H_2 and D_2 in order to compare relaxation times for H_2 and HD and determine differences in the anisotropic intermolecular interactions for the isotopic molecules. The relaxation time for H_2 in D_2 was also determined for comparison with HD in D_2. Relaxation times for HD in CO_2, CHF_3, $CClF_3$, N_2, C_2H_6 and CH_4 were found. Measurements of T_1 for H_2 in these gases, except C_2H_6 and CH_4, have been made (12); thus relaxation times can be compared for H_2 and HD in the same gases over a range of strengths of the anisotropic intermolecular potential.

It was found that at a total gas density of 25.0 amagat T_1 is a linear function of the HD partial pressure over the range of 100% to 30% HD within which accurate measurements could be made. This dependence is shown in Fig. 2. This behavior is the same as that found in previous investigations of H_2 relaxation times in mixtures with other gases (12, 13). Relaxation times for HD and H_2 extrapolated to infinite dilution in the solvent gases are given in Table II with the values for pure HD and H_2. The results obtained by Johnson and Waugh (12) and Williams (13) are also shown. Previous determinations of T_1/ρ in pure H_2 (12, 15, 14, 13) yield values between 0.10 and 0.13 msec./amagat. Our value of 0.114 msec./amagat falls within this range. The accuracy of our T_1 measurements is estimated to be $\pm$ 5% or better.

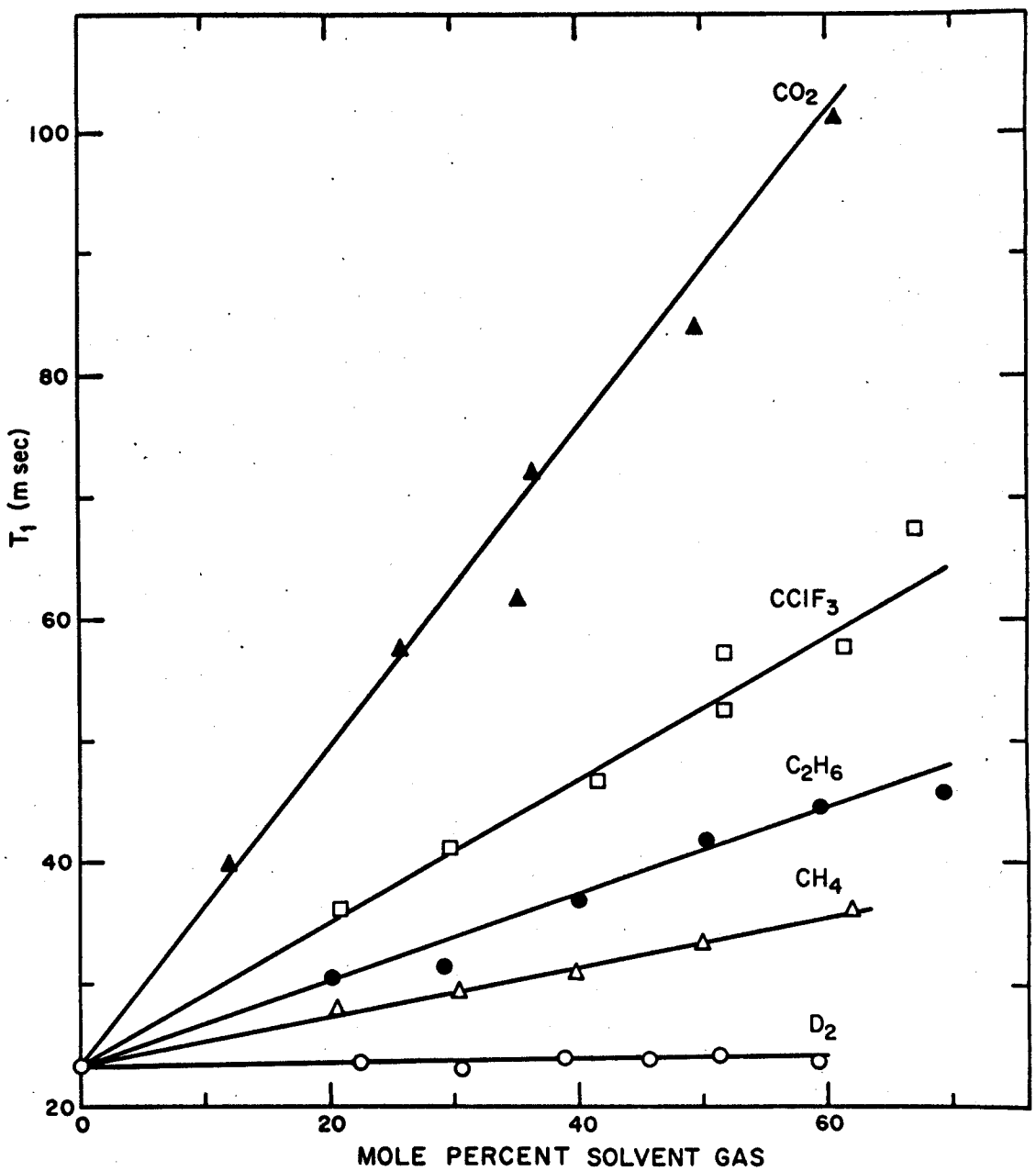

Fig. 2. Dependence of the HD proton T_1 upon composition of mixtures

TABLE II

Relaxation Times T_2, and Transition Probabilities per Collision W, for H_2 and HD at Infinite Dilution in Solvent Gases[a]

	H_2		HD		
Solvent	T_1 (msec.)	W_{H_2}	T_1 (msec.)	W_{HD}	W_{H_2}/W_{HD}
H_2	2.64[c]	0.019[c]			
	2.85	0.0194	23.3	0.0511	0.380
HD			23.3	0.0571	
D_2	2.98	0.0234	24.9	0.0637	0.367
CH_4			43.5	0.102	
N_2	9.6[c]	0.071[b]	47.3	0.119	0.597
	12.7[d]	0.091[d]			0.76
C_2H_6			58.7	0.138	
$CClF_3$	20.9[c]	0.111[b]	82.1	0.150	0.740
CO_2	56.8[c]	0.337	154	0.314	1.07
CHF_3	78.3[c]	0.486[b]	ca. 202	ca. 0.44	ca. 1.1

[a] At 29°C and 25.0 amagat.

[b] Reference 12.

[c] Calculated from data in reference 12.

[d] Calculated from data in reference 13.

In the case of HD in CHF_3 it was found that T_1 was not linear in the HD partial pressure but the plot of T_1 vs. percent CHF_3 was concave downward. Above 50% CHF_3 the values for T_1 were below those for HD in CO_2 at the same concentration. This behavior may be caused by association of CHF_3 or by the poorer magnetic field homogeneity at the time the CHF_3 experiments were performed. The value of T_1 given in Table II was obtained by extrapolating the tangent to the curve at low CHF_3 concentrations where these effects should be small.

Although a complete interpretation of the results requires the application of a detailed theory, much information can be obtained using the Schwinger formula. As discussed previously, T_1 can be described by one correlation time in the case of strong collisions such as those between hydrogen and CO_2. If the collisions are weaker τ_1^J and τ_2^J can not be assumed to be equal and independent of J but the strong collision approximation still provides a useful basis for comparison of T_1 for hydrogen diluted in different gases.

We assume that the collision time, τ_c, is given by the kinetic gas theory for hard spheres

$$\tau_c^{-1} = ND^2 \left(\frac{8\pi kT}{\mu} \right)^{\frac{1}{2}} \tag{17}$$

where N is the number of molecules per unit volume, D is the collision diameter

$$D = \frac{D_H + D_X}{2} \tag{18}$$

and D_H and D_X are the classical Lennard-Jones diameters (31 p. 1110, 32). In the strong collision limit the probability per collision, W, for "an appreciable reorientation of the molecule to occur" (19) is defined by

$$W\tau = \tau_c \tag{19}$$

where τ is the correlation time. Values of W are shown in Table II. The value of W for H_2 in CO_2 is the same as that for HD in CO_2 within experimental error and confirms that the collisions are strong. For W less than that in CO_2 the ratio W_{H_2}/W_{HD} decreases with decreasing W as the transition probability becomes more dependent on the details of the intermolecular interactions.

The assumption of equal correlation times is not valid in the case of weak collisions as in pure HD and H_2. This may explain the larger W for pure HD compared with pure H_2. If we assume $\tau_1^J = \tau_2^J = \tau$, in HD 94% of the contribution to $1/T_1$ comes from the spin-rotational interaction, but in H_2 most of the contribution (64%) is from the dipole-dipole interaction. Thus T_1 depends primarily on τ_1 in HD but T_1 for H_2 is chiefly determined by τ_2. The Bloom-Oppenheim theory predicts (20) that τ_2 is less than τ_1, therefore the smaller W_{H_2} is expected.

The displacement of the center of mass from the charge center of the HD molecule increases the strength of the anisotropic intermolecular interaction enough to explain some of the increase in W over that for H_2. The effect of the center of mass displacement is easily demonstrated using the Morse potential function for the interaction between H_2 and a spherically symmetric molecule or atom (33),

$$V(r,\theta) = D \exp[-\alpha(r-r_o)] - 2D \exp[-\alpha(r-r_o)/2] + \beta D \exp[-\alpha(r-r_o)] P_2(\cos\theta) \quad (20)$$

where for H_2 or D_2 the constants are $D = 1.1 \times 10^{-4}$, $\alpha = 1.87$, $r_o = 6.4$, and $\beta = 0.110$ in atomic units (1). The interaction potential for HD can be obtained from Eq. 20 by expressing the intermolecular distance r and orientation θ at the molecular midpoint in terms of the distance r' and orientation θ' at the center of mass. If only the first order terms are retained we have for HD

$$\begin{aligned} V(r',\theta') = {} & D \exp[-\alpha(r'-r_o) - 2D \exp[-\alpha(r'-r_o)/2] \\ & + \beta D \exp[-\alpha(r'-r_o)] P_2(\cos\theta') \\ & + \frac{\alpha^2 d^2}{3} D \exp[-\alpha(r'-r_o)] P_2(\cos\theta') \\ & - \frac{\alpha^2 d^2}{6} D \exp[-\alpha(r'-r_o)/2] P_2(\cos\theta') \\ & + \alpha d D \left\{ \exp[-\alpha(r'-r_o)] - \exp[-\alpha(r'-r_o)/2] \right\} P_1(\cos\theta') \end{aligned} \quad (21)$$

where $d = 0.1236\ A^o = 0.232$ a.u. is the distance from the HD center of mass to the charge center. The derivation of Eq. 21 is outlined in Appendix IV. Note that the first three terms are the same as the terms in Eq. 20 for H_2. The other terms arise from the isotropic part of the H_2 intermolecular potential. For the odd degree Legendre polynomials, the matrix elements between states having the same J vanish. Thus the terms in $P_1(\cos\theta')$ only induce ΔJ transitions and do not contribute

to the nuclear spin relaxation. The terms that induce Δm_J transitions within a J manifold are those involving $P_2(\cos \theta')$. An indication of the effect of the HD center of mass displacement on the rotational transition probability can be obtained by calculating the square of the ratio of the sum of coefficients of $P_2(u)$ in Eqs. 20 and 21 at a reasonable internuclear distance. At $r = r_o$ and $r' = r_o$ this is

$$\left(\frac{\beta + \frac{\alpha^2 d^2}{3} - \frac{\alpha^2 d^2}{6}}{\beta} \right)^2 = \left(\frac{0.142}{0.110} \right)^2 = 1.7$$

which makes a significant contribution to the observed ratio W_{HD}/W_{H_2} of 2.94.

Bloom has pointed out (22) that the most probable collisions for which J changes are resonant collisions, in which molecules interchange rotational energy. These resonant collisions cannot occur between hydrogen molecules containing different isotopes because the rotational energy differences for the allowed transitions are not the same. Thus if ΔJ transitions were important for nuclear spin relaxation we would expect W for pure HD or H_2 gas to be larger than W for collisions of HD or H_2 with different isotopic hydrogen molecules. We find that the values of W are nearly the same for HD colliding with H_2, HD, and D_2. Similarly, W for H_2/H_2 collisions is nearly the same as W for H_2/D_2 collisions. Although accurate measurements of the H_2 linewidth in mixtures of H_2 and HD could not be made, it was found that T_1 was approximately the same as in pure H_2. Therefore resonant collisions must contribute little to the relaxation.

It is also seen that HD is approximately as effective as H_2 or D_2 in inducing rotational transitions in collisions with other molecules, although in HD the center of mass is displaced from the charge center and there is no symmetry restriction prohibiting $\Delta J = 1$ transitions.

APPLICATION OF THE BLOOM-OPPENHEIM THEORY TO HD

The difference in T_1 for H_2 and HD cannot be quantitatively explained with the Schwinger theory and a more detailed theory must be used. We will discuss the application of the Bloom-Oppenheim theory to HD.

By substituting Eqs. 9 and 10 into Eqs. 2 and 3 and averaging over the rotational states by Eq. 14 we obtain

$$\frac{1}{T_1} = \left[\rho a^4 (2\pi\beta\mu_{H_2})^{\frac{1}{2}} K_{H_2}\right]^{-1} \hbar^2 \sum_{J \text{ even}} P_J J(J+1)(2J-1)(2J+3)$$

$$\times \left[\frac{\gamma_H^2 H'^2}{3} + \frac{\gamma_H^4 \hbar^2}{4R^6(4J^2+4J-7)}\right] \qquad (22)$$

where $K_{H_2} = k_o + k_1$; $k_o = 6\pi I^{(1)}(2)/5$ arises from $H_R^{(1)}$ and $k_1 = 0.134\, C_{H_2} I^{(2)}(4)$ arises from the intermolecular quadrupole-quadrupole interaction.

For HD

$$\frac{1}{T_1} = \left[\rho a^4 (2\pi\beta\mu_{HD})^{\frac{1}{2}} K_{HD}\right]^{-1} \hbar^2 \sum_J P_J J(J+1)(2J-1)(2J+3)$$

$$\times \left[\frac{\gamma_H^2 H_H'^2}{3} + \frac{4\gamma_H^2 \gamma_D^2 \hbar^2}{27 R_{HD}^6 (4J^2+4J-7)}\right] \qquad (23)$$

If the experimental values of T_1 for H_2 and HD are used in Eqs. 22 and 23 it is found that $K_{HD} = 4.43\ K_{H_2}$. The value of K_{H_2} has been determined (20) from the data of Lipsicas and Hartland (14) to be 8.8×10^{24} sec^{-2}. Thus we find that

$$K_{HD} = 4.43 \times (8.8 \times 10^{24}\ sec^{-2}) = 39.0 \times 10^{24}\ sec^{-2}$$

We can calculate K_{HD} from the HD intermolecular potential for comparison with this value of K_{HD}. The HD intermolecular potential can be determined as before by expressing the intermolecular distance and orientation at the center of charge in terms of the distance and orientation at the HD center of mass. It is convenient to use the Lennard-Jones potential to describe the H_2 isotropic interaction:

$$V(r) = 4\epsilon\left[\left(\frac{\sigma}{r}\right)^{12} - \left(\frac{\sigma}{r}\right)^{6}\right] \qquad (24)$$

When Eq. 24 is transformed to the HD center of mass the intermolecular potential is found to be (Appendix IV)

$$V(r',\theta') = 4\epsilon\left[(\sigma/r')^{12} - (\sigma/r')^{6}\right]$$
$$+ 4\epsilon\frac{d}{\sigma}\left[12(\sigma/r')^{13} - 6(\sigma/r')^{7}\right]P_1(\cos\theta')$$
$$+ 4\epsilon\frac{d^2}{\sigma^2}\left\{2(\sigma/r')^{14}[28P_2(\cos\theta') + 11] - \left(\frac{\sigma}{r'}\right)^{8}[16P_2(\cos\theta') + 5]\right\}$$
$$+ 4\epsilon\frac{d^3}{\sigma^3}\left\{(\sigma/r')^{15}\frac{28}{5}[32P_3(\cos\theta') + 33P_1(\cos\theta')]\right.$$
$$\left. - (\sigma/r')^{9}\,8\,[4P_3(\cos\theta') + 3P_1(\cos\theta')]\right\}$$
$$+ \cdots \qquad (25)$$

The terms involving odd degree Legendre polynomials do not contribute to Δm_J transitions and can be disregarded. Thus the terms which contribute to the nuclear spin relaxation are

$$V_2(r',\theta') = 32\epsilon\frac{d^2}{\sigma^2}\left[7(\sigma/r')^{14} - 2(\sigma/r')^{8}\right]P_2(\cos\theta') \qquad (26)$$

The angle dependence is the same as that in the anisotropic potential $\mathcal{H}_R^{(1)}$ for H_2 and the contribution of Eq. 26 to K_{HD} is found by substituting the coefficient of $P_2(\cos\theta')$ for $b^{(1)}(au)$ in Eq. 12 and multiplying the integral by $6\pi/5$. By interpolating between tabulated values (20) for $I^{(1)}(2)$ we find that the contribution to K_{HD} is 2.2×10^{24} sec^{-2} at 29°C.

Similarly we transform the H_2 anisotropic intermolecular potential

$$\mathcal{H}_R^{(1)}(r,\theta) = \frac{k}{r^{19}}P_2(\cos\theta) \qquad (27)$$

to the HD center of mass and obtain (Appendix IV)

$$\mathcal{H}_R^{(1)}(r',\theta') = \frac{k}{r'^{19}}\left\{P_2(\cos\theta') + \frac{d}{r'}\frac{1}{5}\left[32P_1(\cos\theta') + 63P_3(\cos\theta')\right] + \frac{d^2}{r'^2}\left[\frac{96}{5} + \frac{225}{2}P_2(\cos\theta') + \frac{414}{5}P_4(\cos\theta')\right] + \cdots\right\} \quad (28)$$

We can again disregard the odd degree Legendre polynomials and consider only the terms involving $P_2(\cos\theta')$ and $P_4(\cos\theta')$. The $P_4(\cos\theta')$ term leads to a different J dependence for the nuclear spin relaxation and therefore cannot be used to calculate a contribution to K_{HD} as defined in Eq. 23. In order to simplify the calculation we will assume that the contribution of this term is the same as $(225\ kd^2/2r'^{21})\ P_2(\cos\theta')$. The contributions of these terms are small so that this approximation will have little effect on the final results. After extrapolating the tabulated values (20) to evaluate the Integral 12 with $b^{(q)}(au) = 225\ kd^2/r'^{21}$ the contribution to K_{HD} is found to be $1.5 \times 10^{24}\ sec^{-2}$. The total contribution of the potential 28 to K_{HD} is the same as the contribution of Eq. 27 to K_{H_2} plus $1.5 \times 10^{24}\ sec^{-2}$. The contribution of the quadrupole-quadrupole interaction to K_{H_2} is small at room temperature and we will neglect the effect of the center of mass displacement.

From the results of the above calculations we find $K_{HD} = K_{H_2} + 2.2 \times 10^{24}\ sec^{-2} + 1.5 \times 10^{24}\ sec^{-2} = 12.5 \times 10^{24}\ sec^{-2}$. This value differs by a factor of three from the value calculated from the experi-

mental relaxation time. The assumptions introduced in applying the Bloom-Oppenheim theory may be responsible for this large discrepancy. The Lennard-Jones potential may not adequately represent the isotropic intermolecular potential for hydrogen and therefore its contribution to the anisotropic part of the HD intermolecular potential may be too low. Other isotropic intermolecular potential functions would contribute differently to K_{HD} and this provides a means for testing the form of these potentials. We have assumed that the contribution of ΔJ transitions to the HD proton spin relaxation is negligible. However the transition probability for ΔJ transitions is much larger in HD than in $H_2(l)$ and this assumption may not be valid.

REFERENCES

1. C. G. Sluijter, H. F. P. Knaap, and J. J. M. Beenakker, Physica, 31, 915 (1965).
2. R. Holmes, G. R. Jones, N. Pusat, W. Tempest, Trans. Faraday Soc., 58, 2342 (1962).
3. E. A. Mason, J. Chem. Phys., 39, 522 (1963).
4. C. H. Townes, A. L. Schawlow, "Microwave Spectroscopy," McGraw-Hill Book Co., Inc., 1955.
5. J. Fiutak and J. Van Kranendonk, Can. J. Phys., 41, 21 (1963).
6. R. G. Gordon, J. Chem. Phys., 42, 3658 (1965).
7. J. P. Toennies, Disc. Faraday Soc., 33, 96 (1962).
8. A. Abragam, "The Principles of Nuclear Magnetism," Oxford University Press, London, 1961.
9. N. F. Ramsey, "Molecular Beams," Chap. III, Oxford University Press, London, 1961.
10. M. Bloom, Physica, 23, 237 (1957).
11. M. Lipsicas and M. Bloom, Can. J. Phys., 39, 881 (1961).
12. C. S. Johnson, Jr. and J. S. Waugh, J. Chem. Phys., 36, 2266 (1962).
13. D. L. Williams, Can. J. Phys., 40, 1027 (1962).
14. M. Lipsicas and A. Hartland, Phys. Rev., 131, 1187 (1963).
15. G. Widenlocher, E. Dayan, and B. Vodar, Compt. Rend., 256, 2584 (1963).
16. N. Bloembergen, E. M. Purcell, and R. V. Pound, Phys. Rev., 73, 679 (1948).

17. G. T. Needler and W. Opechowski, Can. J. Phys., 39, 870 (1961).

18. I. Oppenheim and M. Bloom, Can. J. Phys., 39, 845 (1961).

19. M. Bloom and I. Oppenheim, Can. J. Phys., 41, 1580 (1963).

20. M. Bloom, I. Oppenheim, M. Lipsicas, C. G. Wade, and C. F. Yarnell, J. Chem. Phys., 43, 1036 (1965).

21. C. P. Slichter, "Principles of Magnetic Resonance," Chap. 5, Harper and Roe, New York, 1963.

22. B. D. N. Rao and L. R. Anders, Phys. Rev., 140, A 112 (1965).

23. J. M. Anderson, Mol. Phys., 8, 505 (1964).

24. A. G. Redfield, IBM J. Research Develop., 1, 19 (1957).

25. W. E. Quinn, J. M. Baker, J. T. La Tourette, and N. F. Ramsey, Phys. Rev., 112, 1929 (1958).

26. J. H. Freed, J. Chem. Phys., 41, 7 (1964).

27. N. Davidson, "Statistical Mechanics," Chap. 9, McGraw-Hill Book Co., Inc., New York, 1962.

28. J. A. Pople, W. G. Schneider and H. J. Bernstein, "High Resolution Nuclear Magnetic Resonance," Chap. 10, McGraw-Hill Book Co., Inc., New York, 1959.

29. A. L. Van Geet and D. N. Hume, Anal. Chem., 37, 979 (1965).

30. A. Fookson, P. Pomerantz, and E. H. Rich, J. Res. NBS, 47, 31 (1951).

31. J. O. Hirschfelder, C. F. Curtiss, and R. B. Bird, "The Molecular Theory of Gases and Liquids," 2nd ed., John Wiley and Sons, Inc., New York, 1954.

32. G. A. Miller and R. B. Bernstein, J. Phys. Chem., 63, 710 (1959).

33. K. Takayanagi, Supplement of the Prog. Theor. Phys., no. 25 (1963).

A P P E N D I X E S

I. THIN LAYER REVERSE CURRENT CHRONOPOTENTIOMETRY OF A REACTING SPECIES

Consider the situation depicted graphically in Figure 1 of Part II: oxidation of a species, R, for time t_f, interruption of current flow for time t_d, and reduction of species Ox which undergoes an irreversible first-order reaction to an electrochemically inert species Z:

$$R - ne \rightleftharpoons Ox$$

$$Ox \xrightarrow{k} Z$$

It is desired to calculate the concentration of Ox in the solution layer at any time.

For $0 < t < t_f$

$$\frac{dC_{ox}}{dt} = \beta - kC_{ox} \tag{1}$$

where C_{ox} is the concentration of Ox and $\beta = i/(nFA\ell)$. Since $C_{ox} = 0$ for $t = 0$, the solution of Equation 1 is

$$C_{ox} = \frac{\beta}{k}(1 - e^{-kt}) \tag{2}$$

For $t_f < t < t_f + t_d$

$$\frac{dC_{ox}}{dt} = -kC_{ox} \tag{3}$$

Letting $t' = t - t_f$, C_{ox} at time $t' = 0$ is, from Equation 2

$$t' = 0,\ C_{ox} = \frac{\beta}{k}(1 - e^{-kt_f}) \tag{4}$$

The solution of Equation 3 is then

$$C_{ox} = \frac{\beta}{k} e^{-kt'} (1 - e^{-kt_f}) \tag{5}$$

For $t_f + t_d < t < t_f + t_d + \tau$

$$\frac{dC_{ox}}{dt} = -\theta\beta - kC_{ox} \tag{6}$$

where θ is the ratio of the current employed in the cathodic process to the current employed in the anodic process. Letting $t'' = t - (t_f + t_d)$, C_{ox} at time $t'' = 0$, is from Equation 5

$$t'' = 0, C_{ox} = \frac{\beta}{k} e^{-kt_d}(1 - e^{-kt_f}) \tag{7}$$

The solution of Equation 6 is then

$$C_{ox} = \frac{\beta}{k} \times \{e^{-kt''} [\theta + e^{-kt_d}(1 - e^{-kt_f})] - \theta\} \tag{8}$$

Finally, the transition time τ, is defined by $C_{ox} = 0$ when $t'' = \tau$. Hence from Equation 8

$$e^{-k\tau} [\theta + e^{-kt_d}(1 - e^{-kt_f})] - \theta = 0 \tag{9}$$

and $$\tau = \frac{1}{k} \ln \left[1 + \frac{1}{\theta} e^{-kt_d} (1 - e^{-kt_f})\right]$$

which leads to Equation 1, Part II for $\theta = 1$.

II. OVERLAP CORRECTION FOR TWO ADJACENT LORENTZIAN LINES

The shape of a Lorentzian line centered at ν_o is given by

$$g(\nu_o - \nu) = \frac{h}{1 + (2/\Delta\nu)^2(\nu_o - \nu)^2}$$

where h is the full height and $\Delta\nu$ is the full width at half height. Consider two Lorentzian lines, each with height h and width $\Delta\nu$, one centered at $\nu = +S/2$ and the other centered at $\nu = -S/2$. The peaks are therefore separated by a distance S. If $(S/\Delta\nu) \lesssim 10$ the lines will overlap appreciably and in measuring linewidths the effect of the adjacent line must be considered. The observed spectrum is given by the sum of the two lines.

$$g(\nu) = g(S/2 - \nu) + g(-S/2 - \nu)$$

$$= h\left[\frac{1}{1 + (2/\Delta\nu)^2(S/2 - \nu)^2} + \frac{1}{1 + (2/\Delta\nu)^2(-S/2 - \nu)^2}\right] \qquad (1)$$

Neglecting the shift of the maxima toward $\nu = 0$ the heights of the two peaks will be

$$g(\pm S/2) = 2h\left[\frac{1 + 2\,(S/\Delta\nu)^2}{1 + 4\,(S/\Delta\nu)^2}\right] \qquad (2)$$

At half height $$g(\nu) = \tfrac{1}{2}\, g(\pm S/2) \qquad (3)$$

From Equations 1, 2 and 3 the values of ν at half height are found to be

$$\nu = \pm \frac{\Delta \nu}{2} \left[\frac{(S/\Delta \nu)^2 B + 1-B \pm \sqrt{1 + 4(S/\Delta \nu)^2 B(1-B)}}{B} \right]^{\frac{1}{2}} \qquad (4)$$

in which $$B = \frac{1 + 2(S/\Delta \nu)^2}{1 + 4(S/\Delta \nu)^2}$$

The observed line width for either line is obtained from the difference in values of ν for that line given by Equation 4. The percent increase in line width of one line due to overlap of the adjacent line is shown in Fig. 1 where the quantity

$$\frac{\text{Observed Line Width} - \Delta \nu}{\Delta \nu} \times 100$$

is plotted vs. $S/\Delta \nu$.

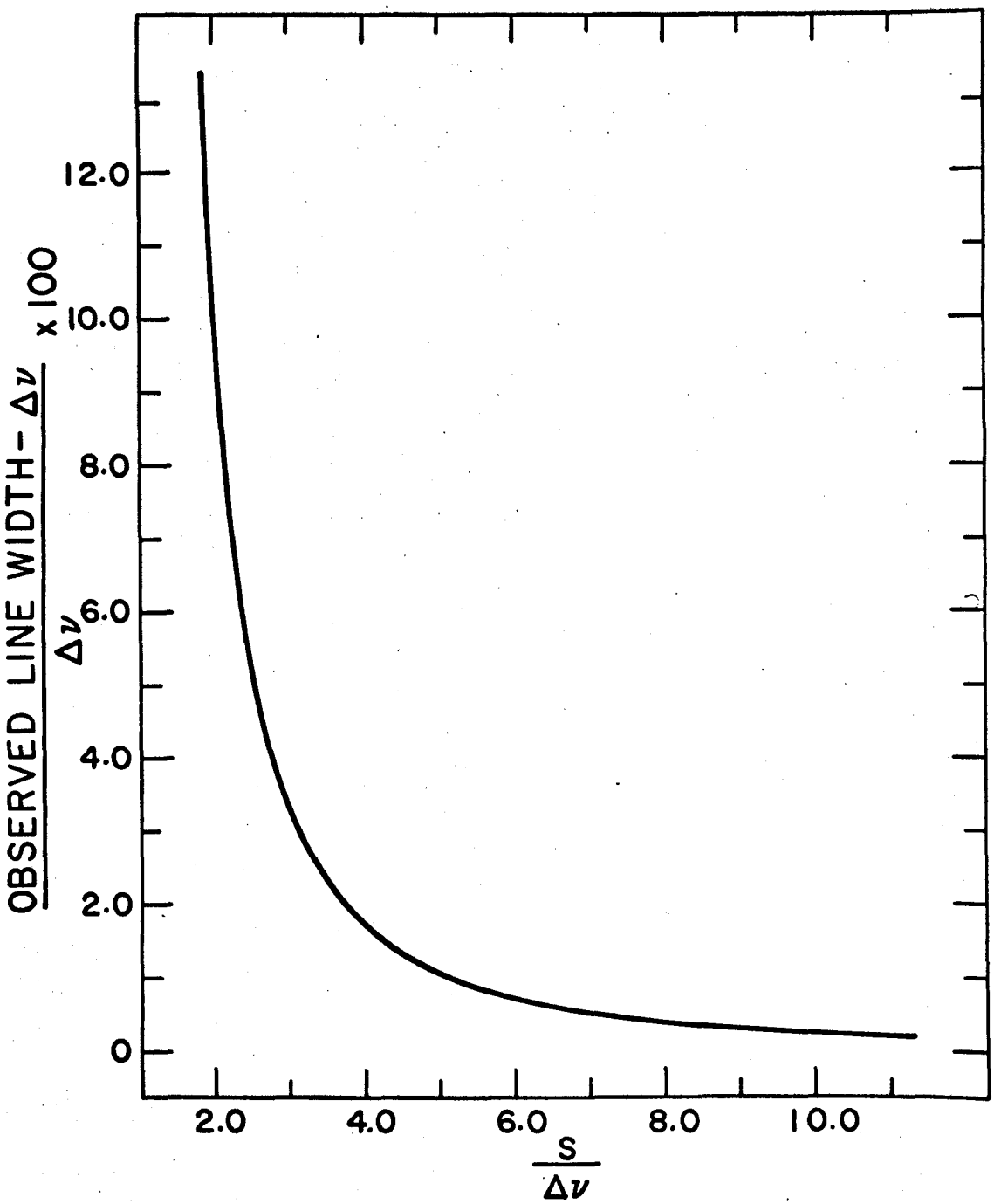

Fig. 1. Increase in half width of a Lorentzian line due to overlap of an identical adjacent line.

III. DIFFUSION RATE OF H_2 ACROSS A NMR SAMPLE TUBE

An estimate of the mean distance of diffusion in time, t, may be obtained from (1)

$$\overline{\Delta X^2} = 2\,Dt$$

where $\overline{\Delta X^2}$ is the mean square displacement and D is the diffusion coefficient. For pure H_2 at 273°K and 1 atm. D = 1.285 $cm^2 sec^{-1}$ (2 p. 581) and at 25 atm. one expects (2 p. 615) that D = 1.285/25. Thus for a displacement of 0.4 cm, approximately the distance across a 5 mm od NMR tube, requires

$$t = \frac{(0.4\text{ cm})^2}{2(1.285/25)\text{ cm}^2\text{sec}^{-1}} \approx 1.7\text{ sec}$$

For H_2 at infinite dilution in heavy gases such as O_2, CO_2, or CH_4 the diffusion coefficient is approximately half that for pure H_2 (2 p. 579) and the time required is ca. 3.3 sec. HD, with a larger mass, would diffuse even more slowly. If the sample is spinning at the usual rate of 25 rps the part of the sample at the tube wall undergoes this same displacement within about 0.02 sec.

REFERENCES

(1) W. J. Moore, "Physical Chemistry," 2nd ed., p. 449, Prentice-Hall, Inc., Englewood Cliffs, 1955.

(2) J. O. Hirschfelder, C. F. Curtiss, and R. B. Bird, "The Molecular Theory of Gases and Liquids," 2nd ed., John Wiley and Sons, Inc., New York, 1954.

IV. INTERMOLECULAR POTENTIAL FOR HD

Morse Potential

The intermolecular potential for H_2 is (1)

$$V(r,\theta) = D \exp[-\alpha(r-r_o)] - 2D \exp[-\alpha(r-r_o)/2] + \beta D \exp[-\alpha(r-r_o)] P_2(\cos\theta)$$

The coordinates r and θ expressed in terms of the corresponding coordinates centered at the HD center of mass are

$$r = (r'^2 - 2dr'\cos\theta' + d^2)^{\frac{1}{2}} \quad (1)$$

$$\cos\theta = \frac{r'\cos\theta' - d}{(r'^2 - 2dr'\cos\theta' + d^2)^{\frac{1}{2}}} \quad (2)$$

where r' is the distance from the HD center of mass to the center of the other molecule, θ' is the angle between the axis of the HD molecule and $\underset{\sim}{r'}$, and d is the distance from the HD center of mass to the charge center. The HD intermolecular potential is obtained by substituting the expressions 1 and 2 for r and $\cos\theta$ in $V(r,\theta)$. The derivation is simplified if we remember the magnitudes of the constants in $V(r,\theta)$ and neglect the unimportant terms that arise. These constants are (2) $D = 1.1 \times 10^{-4}$, $\alpha = 1.87$, $\beta = 0.110$, $d = 0.232$ and $r \gtrsim 6$ in atomic units.

We can expand Eq. 1 in a binomial series to obtain

$$r = r' - d\cos\theta' + \frac{d^2}{2r'} + \cdots \tag{3}$$

The first exponential in the intermolecular potential becomes

$$\exp[-\alpha(r-r_o)] = \exp[-\alpha(r'-r_o)]\exp[\alpha(d\cos\theta' - d^2/2r' + \cdots)] \tag{4}$$

which can be written as

$$\begin{aligned}\exp[-\alpha(r-r_o)] = \exp[-\alpha(r'-r_o)]\,[&(1 + \alpha^2d^2/6 - \alpha^2d^2/2r') \\ &+ (\alpha d - \alpha^2d^3/2r')\,P_1(\cos\theta') \\ &+ (\alpha^2d^2/3)\,P_2(\cos\theta')]\end{aligned} \tag{5}$$

by expanding the last exponential in Eq. 4 and neglecting higher order terms. The term $\exp[-\alpha(r-r_o)/2]$ is obtained from Eq. 5 by replacing α by $\alpha/2$.

Similarly we substitute Eq. 2 into $P_2(\cos\theta)$:

$$P_2(\cos\theta) = \tfrac{1}{2}\left\{3\left[\frac{(r'\cos\theta' - d)}{(r'^2 - 2dr'\cos\theta' + d^2)^{\frac{1}{2}}}\right]^2 - 1\right\}$$

$$= \frac{1}{r^2}\,\tfrac{1}{2}\left\{3r'^2\cos^2\theta' - r'^2 - 4dr'\cos\theta' + 2d^2\right\} \tag{6}$$

We write

$$\frac{1}{r^2} = \frac{1}{r'^2 - 2dr'\cos\theta' + d^2}$$

$$= \frac{1}{r'^2}\left(\frac{1}{1 - 2\frac{d}{r'}\cos\theta' + \frac{d^2}{r'^2}}\right)$$

and use a binomial expansion to get

$$\frac{1}{r^2} = \frac{1}{r'^2}\left(1 + 2\frac{d}{r'}\cos\theta' - \frac{d^2}{r'^2} + 4\frac{d^2}{r'^2} + \cdots\right) \tag{7}$$

by substituting Eq. 7 into 6 and writing the result in terms of the Legendre polynomials we get

$$P_2(\cos\theta) = P_2(\cos\theta') + \frac{6}{5}\frac{d}{r'}\left[P_3(\cos\theta') - P_1(\cos\theta')\right]$$

$$+ \frac{1}{35}\frac{d^2}{r'^2}\left[48\,P_4(\cos\theta') - \frac{55}{3}P_2(\cos\theta') - 9\right]$$

$$+ \cdots \tag{8}$$

After multiplying Eq. 5 by Eq. 8 and neglecting the smaller terms we have

$$\exp\left[-\alpha(r-r_o)\right] P_2(\cos\theta) =$$

$$\exp\left[-\alpha(r'-r_o)\right]\left[P_2(\cos\theta') + (2\alpha d/5 - 6d/5r')\,P_1(\cos\theta')\right.$$

$$\left. + (3\alpha d/5 + 6d/5r')\,P_3(\cos\theta')\right] \tag{9}$$

When Eqs. 9, 5, and the equation for $\exp\left[-\alpha(r-r_o)/2\right]$ are substituted into $V(r,\theta)$ we get for the HD intermolecular potential

$$V(r',\theta') = D \exp[-\alpha(r'-r_o)] - 2D \exp[-\alpha(r'-r_o)/2]$$

$$+ \beta D \exp[-\alpha(r'-r_o)] P_2(\cos\theta')$$

$$+ \frac{\alpha^2 d^2}{3} D \exp[-\alpha(r'-r_o)] P_2(\cos\theta')$$

$$- \frac{\alpha^2 d^2}{6} D \exp[-\alpha(r'-r_o)/2] P_2(\cos\theta')$$

$$+ \alpha d D \exp[-\alpha(r'-r_o)] P_1(\cos\theta')$$

$$- \alpha d D \exp[-\alpha(r'-r_o)/2] P_1(\cos\theta')$$

in which the higher order terms have been neglected.

Lennard-Jones Potential

We write $1/r^n$ in terms of the coordinates centered at the HD center of mass as

$$\frac{1}{r^n} = \frac{1}{r'^n} \frac{1}{\left(1-2\frac{d}{r'}\cos\theta + \frac{d^2}{r'^2}\right)^{n/2}}$$

and use a binomial expansion to obtain

$$\frac{1}{r^n} = \frac{1}{r'^n}\left\{1 + \frac{d}{r'} n P_1(\cos\theta') + \frac{d^2}{r'^2}\frac{n}{3}\left[(n+2)P_2(\cos\theta') + \frac{n-1}{2}\right]\right.$$

$$+ \frac{d^3}{r'^3}\frac{n(n+2)}{5}\left[\frac{(n+4)}{3} P_3(\cos\theta') + \frac{(n-1)}{2} P_1(\cos\theta')\right]$$

$$\left. + \cdots \right\} \qquad (10)$$

The HD intermolecular potential is found by substituting Eq. 10 into the Lennard-Jones potential, in which n = 12 and 6. We get

$$V(r',\theta') = 4\epsilon\,[(\sigma/r')^{12} - (\sigma/r')^{6}]$$

$$+ 4\epsilon\,\frac{d}{\sigma}\left\{12(\sigma/r')^{13} - 6(\sigma/r')^{7}\right\} P_1(\cos\theta')$$

$$+ 4\epsilon\,\frac{d^2}{\sigma^2}\left\{2(\sigma/r')^{14}[28P_2(\cos\theta') + 11] - (\sigma/r')^{8}[16P_2(\cos\theta')+5]\right\}$$

$$+ 4\epsilon\,\frac{d^3}{\sigma^3}\left\{(\sigma/r')^{15}(28/5)[32P_3(\cos\theta') + 33P_1(\cos\theta')\right.$$

$$\left. - (\sigma/r')^{9}\,8[4P_3(\cos\theta') + 3P_1(\cos\theta')]\right\}$$

$$+ \cdots$$

Anisotropic Part of the H_2 Potential

The potential for the interaction of a hydrogen molecule with a spherically symmetric atom or molecule

$$\mathcal{H}_R^{(1)} = \frac{k}{r^{19}} P_2(\cos\theta)$$

is found in terms of the HD coordinates r' and θ' from Eq. 6 for $P_2(\cos\theta)$ and Eq. 10 for $1/r^{19}$. After multiplying the terms on the right hand sides of Eqs. 6 and 10 we find

$$\mathcal{H}_R^{(1)}(r',\theta') = \frac{k}{r'^{19}}\left\{P_2(\cos\theta') + \frac{d}{r'}\,\frac{1}{5}\,[32P_1(\cos\theta') + 63P_3(\cos\theta')]\right.$$

$$+ \frac{d^2}{r'^2}\,[96/5 + (225/2)P_2(\cos\theta') + (414/5)P_4(\cos\theta')]$$

$$\left. + \cdots\right\}$$

REFERENCES

(1) K. Takayanagi, Supplement of the Prog. Theor. Phys., no. 25 (1963).

(2) C. J. Sluijter, H. F. P. Knapp, and J. J. M. Beenakker, Physica, 31, 915 (1965).

P R O P O S I T I O N S

PROPOSITION I

The nuclear magnetic resonance properties of tritium, H^3, are similar to those for the proton. Both nuclei have spin $\frac{1}{2}$ and the NMR frequency of 45.414 Mc at 10,000 gauss for tritium is only slightly higher than the proton frequency of 42.577 Mc. Thus tritium resonance can easily be observed with conventional spectrometers. High resolution tritium NMR of ethylbenzene containing 1 atom % tritium has recently been reported (1). Measurements were made using a 40.000 Mc Varian spectrometer at ca. 8800 gauss. We propose that a study be made of nuclear spin relaxation in H_2^3 gas.

Because both nuclei have spin $\frac{1}{2}$ the relaxation mechanisms are the same in H_2^3 and H_2^1 and the form of the relation for $T_{1,J}$ in tritium gas is identical to that for H_2^1:

$$\frac{1}{T_{1,J}} = \frac{2}{3}\gamma_T^2 H_T'^2 J(J+1)\ \tau_1^J + \frac{6\gamma_T^4\hbar^2 J(J+1)}{R_T^6(2J-1)(2J+3)}\ \tau_2^J$$

The spin-rotation and dipolar coupling constants have not been experimentally determined but these can be calculated from the known values for the other isotopic hydrogen molecules using the vibrational and rotational constants to take into account the effects of zero point vibration (2, 3). We expect the relaxation times for H_2^3 and H_2^1 to be of the same order of magnitude because γ_T and γ_H only differ by ca. 6%.

The intermolecular potentials for H_2^3 and H_2^1 are expected to be identical, however the rotational energy levels of H_2^3 are not as

far apart as those of H_2^1 and this leads to different rotational level populations at a given temperature. Therefore a comparison of the relaxation times for H_2^1 and H_2^3 from near the boiling points to room temperature would provide a useful test of the theories for nuclear spin relaxation. At low temperatures, such that only the first rotational state contributes significantly to the hydrogen spin relaxation, the correlation times τ_1^1, and τ_2^1 can be calculated directly from the H_2^1 and H_2^3 relaxation times.

It would also be desirable to measure T_1 for tritium in mixtures with rare gases for comparison with T_1 of H_2^1 in the same gases. Measurements on mixtures of tritium with other gases would be difficult due to the chemical reactivity of tritium (4).

These experiments can be performed with less than 20 ml of H_2^3 gas, which is less than 50 curies. Tritium gas can be purchased from Oak Ridge National Laboratory for $2.00/curie; therefore the cost of the experiments would be low. Tritium emits low energy β-radiation and ordinary containers furnish adequate radiation shielding. The safety precautions required in handling tritium involve preventing escape of the gas to the atmosphere.

REFERENCES

1. G. V. D. Tiers, C. A. Brown, R. A. Jackson, and T. N. Lahr, J. Am. Chem. Soc., 86, 2526 (1964).
2. N. F. Ramsey, Phys. Rev., 87, 1075 (1952).
3. S. I. Chan, D. Ikenberry, and T. P. Das, Phys. Rev., 135, A960 (1964).
4. R. J. Kandel, J. Chem. Phys., 41, 2435 (1964).

PROPOSITION II

The diffraction of a beam of slow electrons can provide much information about the surface properties of materials. The wave length for a 150 volt electron beam is 1 Å, the same order of magnitude as X-rays. However slow electrons do not penetrate much beyond the first atomic layer and the diffraction pattern produced is due to the two-dimensional surface structure. Thus the spatial arrangements of the individual surface atoms can be determined and changes in the surface structure observed (1).

Although the first experiments involving low energy electron diffraction were reported (2) in 1927 very little research was done using this technique until about 1960. A renewal of interest in this method was brought about by the recent advances in high vacuum technology and by the development of a better method for observing the diffraction pattern. Commercial apparatus which displays the diffraction pattern on a fluorescent screen is now available. This permits studies to be made of changes in surface structure with time.

The studies of nickel surfaces illustrate the type of information that can be obtained using low energy electron diffraction. It is found that the clean surface has about the same structure as the bulk material. The adsorption of oxygen on the surface is found to cause rearrangement of the surface nickel atoms and the structure of the reconstructed surface depends on the crystal face observed. Adsorption of half a monolayer of hydrogen atoms causes a complete rearrangement

of the nickel atoms on a (110) face (3). This reconstruction of surfaces by adsorption of gases is of obvious significance for chemical reactions occurring at surfaces, particularly for catalysis (3).

An important class of chemical reactions at surfaces is electrochemical reactions, occurring at electrodes in solution. The rate of electron transfer from the electrode to a species in solution may depend dramatically on the surface condition of a solid electrode (4). For example the reduction of vanadium(V) has been found to be much more reversible at a freshly oxidized and reduced platinum electrode than at the same electrode after allowing it to age in the solution. The reduction is also less reversible if the electrode is first electrochemically oxidized and the oxide removed by treatment with HCl (5). It was suggested that these effects are due to microscopic roughening by the process of oxidizing and reducing the electrode surface, and that aging the electrode allows the surface atoms to rearrange to a less electrochemically active configuration (or allows the surface to adsorb contaminants from the solution to make it less active) (4, 5).

We propose that the surface structure of metals such as platinum, iridium, rhodium, palladium, and gold be investigated by low energy electron diffraction and a comparison made between the surface structure and the electrochemical properties of the different crystal surfaces. The electron diffraction study should include the effect on the surface structure of adsorbed water, oxygen, and hydrogen and the change in structure of an oxidized surface after reduction with hydrogen. It would also be of interest to investigate the effect of water

adsorption on the clean surfaces and on the oxidized and reduced surfaces. This work would help explain the irreversibility of electrode reactions at oxidized electrodes and the increased reversibility of electrode reactions at freshly oxidized and reduced electrodes.

A study of platinum surfaces has been made (6). Adsorption of O_2 was found to lead to a rearrangement of the top layers of platinum atoms on all three crystal faces. When the oxygen structure of the (111) face was reacted with hydrogen at room temperature all oxygen was immediately removed and a more complex structure formed over a period of approximately an hour. Removal of oxygen from the oxidized (111) surface by reduction with hydrogen or carbon monoxide left the rearranged platinum surface unchanged. However, heating the sample to 200°C returned the structure to normal. The adsorption of water was not studied.

REFERENCES

1. A. U. MacRae, Science, 139, 379 (1963).
2. C. J. Davisson and L. H. Germer, Phys. Rev., 30, 705 (1927).
3. L. H. Germer, Physics Today, 17, no. 7, p. 19 (1964).
4. F. C. Anson, Anal. Chem., 33, 935 (1961).
5. F. C. Anson and D. M. King, Anal. Chem., 34, 362 (1962).
6. C. W. Tucker, Jr., J. Appl. Phys., 35, 1897 (1964).

PROPOSITION III

Many investigations have been made of proton spin relaxation in aqueous solutions of paramagnetic ions such as Fe^{+3} and Mn^{+2} (1) but few studies have been reported for solutions of molecular free radicals. Work has been reported on nuclear relaxation in nonaqueous solutions of 2,2-diphenyl-1-picrylhydrazyl and di-t-butylnitroxide (2). There are few known stable, water soluble free radicals and this may explain the scarcity of studies in aqueous solutions.

Recently two families of nitroxide radicals have been reported (3). These are of the form

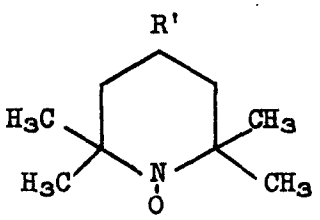

and

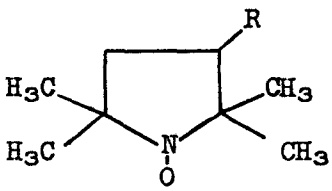

where R' is a group such as =O, =N-OH, or $-C_2H_5$ and R may be a group such as -COOH or $-CONH_2$. These free radicals are stable and several of them are readily soluble in water. We propose that a study be made of the water proton spin relaxation in aqueous solutions of these free radicals and of aqueous solutions of the nitrosyldisulfonate ion, $ON(SO_3)_2^{=}$.

Nuclear spin relaxation in solutions containing paramagnetic species can be explained in terms of two mechanisms (1). One is the relaxation due to the nucleus-electron dipole-dipole interaction modulated by the relative rotational and translational motion of the solvent

molecules and the paramagnetic ions or molecules. This is found to be the dominant mechanism in solutions of many paramagnetic ions (1). A detailed theory has been presented by Solomon (4) which explains the observed equality of T_1 and T_2 and the linear dependence of $1/T_1$ on the concentration of the paramagnetic species.

The other mechanism that contributes to the proton spin relaxation is the scalar coupling of the form $A\ \underset{\sim}{I}\cdot\underset{\sim}{S}$. This interaction can arise if the wave function of the unpaired electron extends to protons in the water molecules. The correlation time τ_e for this mechanism is given by

$$\frac{1}{\tau_e} = \frac{1}{\tau_s} + \frac{1}{\tau_h}$$

where τ_s is the electron spin-lattice relaxation time and τ_h is the time the proton of a solvating water molecule remains close to the paramagnetic species. This mechanism contributes to proton relaxation in Mn^{+2} solutions and explains the large ratio of T_1/T_2. Overhauser nuclear polarization requires an interaction $A\ \underset{\sim}{I}\cdot\underset{\sim}{S}$ and the Overhauser effect observed in aqueous solutions of $ON(SO_3)_2^{=}$ shows that this makes an appreciable contribution to the nuclear relaxation.

From this discussion we see that a study of relaxation times in solutions of free radicals will yield information about molecular motion and solvation of the radical molecules. A comparison of the relaxation times in solutions of the $ON(SO_3)_2^{=}$ ion with relaxation times in solutions of nitroxide radicals which would be only weakly ionized would therefore be of considerable interest. Relaxation times are dependent

on the temperature and nuclear resonance frequency and this dependence is an important source of information. Association of free radicals in the solution would also affect the relaxation times and a comparison of the observed relaxation times with those expected if only individual radicals existed in solution would indicate the degree of association. Many different nitroxide radicals of the types shown could be prepared (3). Thus one can study solvation, molecular motion, and association of a variety of molecules containing substituents of interest.

REFERENCES

1. J. A. Pople, W. G. Schneider, and H. J. Bernstein, "High Resolution Nuclear Magnetic Resonance," Chap. 9, McGraw-Hill Book Co., Inc., New York, 1959.
2. H. S. Gutowsky and J. C. Tai, J. Chem. Phys., 39, 208 (1963).
3. E. G. Rozantzev and N. B. Neiman, Tetrahedron, 20, 131 (1964); 21, 491 (1965).
4. I. Solomon, Phys. Rev., 99, 559 (1955).

PROPOSITION IV

The hyperfine structure for the natural abundance of N^{15} and S^{33} in the nitrosyldisulfonate ion, $ON(SO_3)_2^{=}$, has been observed in the electron spin resonance spectra (1). The hyperfine interaction with O^{17} was not observed because of the low natural abundance of O^{17}.. We propose that O^{17} enriched $ON(SO_3)_2^{=}$ be prepared and the nitrosyl O^{17} hyperfine interaction be observed.

The hydroxylaminedisulfonate ion is prepared in almost quantitative yield by reduction of nitrous acid with HSO_3^- at 0°C:

$$2HSO_3^- + HNO_2 \longrightarrow HON(SO_3)_2^{=} + H_2O$$

Oxidation of $HON(SO_3)_2^{=}$ with a reagent such as PbO_2, AgO_2, or alkaline MnO_4^- yields $ON(SO_3)_2^{=}$ (2, 3). The nitrosyldisulfonate ion is stable for days or weeks in a neutral or alkaline solution at room temperature. Water enriched to 3% O^{17} and O_2 enriched to 4% O^{17} are available. These can be used to prepare O^{17} enriched NO_2^- by exchange in a solution of NO_2^- or by the reactions (4):

$$2NO + \tfrac{1}{2}\, O_2 \longrightarrow N_2O_3$$

$$N_2O_3 + 2OH^- \longrightarrow 2NO_2^- + H_2O$$

The enriched NO_2^- can then be used to prepare $ON(SO_3)_2^{=}$ by the usual procedure.

The isotropic part of the hyperfine interaction is observed in solutions of free radicals. This is proportional to the probability

$|\psi(0)|^2$ of finding the electron at the nucleus and therefore provides information on the electronic structure of the molecule. The theories (5, 6) for the electronic structure of $ON(SO_3)_2^{=}$ can then be tested by comparing their predictions with the observed hyperfine coupling. The hyperfine interaction of oxygen in the $>NO$ group is of interest because a three electron bond is involved.

REFERENCES

1. J. J. Windle and A. K. Wiersema, J. Chem. Phys., 39, 1139 (1963).
2. S. Yamada and R. Tsuchida, Bull. Chem. Soc. of Japan, 32, 721 (1959).
3. D. M. Yost and H. Russell, Jr., "Systematic Inorganic Chemistry of the Non-metallic Elements of the 5th and 6th Groups," p. 91, Prentice-Hall, New York, 1946.
4. M. C. Sneed and R. C. Brasted, Eds., "Comprehensive Inorganic Chemistry," Vol. V, D. Van Nostrand Co., Princeton, 1956.
5. J. W. Linnett and R. M. Roseberg, Tetrahedron, 20, 53 (1964).
6. S. Tan, Hau Hsueh Tung Po, 531 (1963).

PROPOSITION V

Typical surfactants are molecules with molecular weight of about 300 and having a polar solubilizing group and a non-polar hydrophobic group. An example is sodium dodecyl sulfate, $CH_3(CH_2)_{10}CH_2\text{-}SO_3Na$. In solutions at low concentrations these exist as solvated molecules or ions. Above a certain concentration micelles, or aggregates of the surfactant molecules, form. The concentration at which this occurs is called the critical micelle concentration, CMC. By light scattering and diffusion measurements on these systems it is found that the micelles contain about 100 units and are narrowly dispersed in size. Above the CMC the micelle concentration increases approximately linearly with the surfactant concentration and the monomer concentration decreases slightly (1).

The structure of these micelles is still in dispute. The simplest and most widely accepted structure is the spherical micelle with the polar heads of the surfactant on the surface of the sphere and exposed to the water. However there is good evidence that micelles are lamellar, cylindrical or rod shaped, or disc shaped (2).

The increased solubility of a substance in a surfactant solution relative to its solubility in the pure solvent is called solubilization (2). Three types of solubilization have been proposed. In one case the solubilizate is depicted as being dispersed in the interior of the micelles away from the polar groups. In another type the solubilizate molecules are orientated like the surfactant molecules in the

micelle with their polar groups on the outside. A third type of solubilization involves adsorption of the solubilizate on the surface of the micelles (2, 3).

In order to obtain information about the details of micelle structure and the distribution of solubilized molecules in the micelle this author has undertaken a study of proton spin relaxation in surfactant solutions containing paramagnetic species. Some preliminary results will be discussed here and future work proposed. This work was undertaken in connection with an ESR study by Dr. O. Hayes Griffith.

Proton linewidths were measured in solutions of 5 to 10% sodium dodecyl sulfate containing the radical

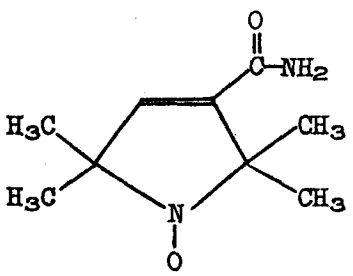

I

in an amount equivalent to one molecule per micelle. In 5% sodium dodecyl sulfate almost all the surfactant is aggregated to form micelles. The proton linewidth of solubilized benzene in these solutions was also observed. The benzene concentration was about 25 molecules per micelle. The resonance of both the H_3C- and $-CH_2$-protons in the hydrocarbon chain can be observed in H_2O, and in D_2O the $-CH_2-SO_3^-$ protons can be observed.

As would be expected at these low free radical concentrations the H_2O linewidth is not significantly increased. However the line-

widths for the dodecyl sulfate protons are increased by 3.0 cps. Thus the free radical is closely associated with the surfactant and presumably contained in the micelles. Molecular motion is rapid compared with the relaxation times. Therefore the linewidths for all three types of dodecyl sulfate protons are increased about the same amount. The linewidth for the benzene resonance is only increased by about 1.3 cps. Thus the radical is interacting less strongly with benzene than with the surfactant. This may indicate that benzene and the free radical are usually not solubilized in the same micelles. Another free radical,

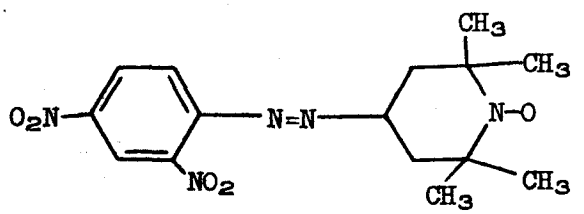

II

has a similar effect on the relaxation times.

In order to satisfactorily explain these observations accurate relaxation time measurements are necessary. These should be made over a range of concentrations and compared with the relaxation times for nonaqueous solvents containing the radicals. The size of the micelles is known (1, 3). Therefore information can be obtained on the distribution and motion of the solubilized species in the micelles as well as the micelle shape. Surfactants which are known to form different sizes or types of micelles, and free radicals or hydrocarbons which are known to be solubilized differently (3) should be investigated.

If the surfactant is an electrolyte the micelles carry a considerable net charge and counter-ions are associated with it. For sodium dodecyl sulfate about 50% of the sodium ions are associated with the micelle. This suggests that the micelle structure can be studied by measuring relaxation times for the surfactant in solutions containing paramagnetic ions such as Cu^{++} and Ni^{++}. The relaxation times for solubilized materials in these solutions would also provide information on their distribution in the micelle.

Surfactants in nonaqueous solvents such as benzene and other hydrocarbon solvents form micelles with their polar groups directed toward the interior and the hydrophobic chains extending into the solvent (2). These are capable of solubilizing water. We propose that a study be made of proton relaxation by paramagnetic species in these systems. Here we can add free radicals not soluble in water, such as 2,2-diphenyl-1-picrylhydrazyl and study proton relaxation of the surfactant and of water solubilized by the surfactant. Relaxation times of solutions containing paramagnetic ions in the solubilized water should also provide information on the micelle structure.

REFERENCES

1. A. W. Adamson, "Physical Chemistry of Surfaces," Interscience Publishers, Inc., New York, 1960.
2. L. I. Osipow, "Surface Chemistry," Reinhold Publishing Corp., New York, 1962.
3. A. M. Schwartz, J. W. Perry and J. Berch, "Surface Active Agents and Detergents," Vol. II, Interscience Publishers, Inc., New York, 1958.